UNIVERSITÀ DEGLI STUDI DI MILANO
SCUOLA DI SPECIALIZZAZIONE IN FISICA MEDICA
FACOLTÀ DI MEDICINA E CHIRURGIA

KNOWLEDGE-BASED AUTOMATIC PLANNING OPTIMIZATION FOR WHOLE BREAST IRRADIATION

Relatore
Prof.ssa Cristina Lenardi

Correlatori
Dr. Claudio Fiorino
Dr.ssa Roberta Castriconi

Controrelatori
Prof.ssa Stefania Pallotta
Dr. Lorenzo Placidi

Tesi di Specializzazione di
Pier Giorgio Esposito
Matr.S62562

Anno Accademico 2019/2020

UNIVERSITY OF MILANO
POSTGRADUATE SCHOOL OF MEDICAL PHYSICS
FACULTY OF MEDICINE

KNOWLEDGE-BASED AUTOMATIC PLANNING OPTIMIZATION FOR WHOLE BREAST IRRADIATION

Supervisor
Prof. Cristina Lenardi

Co-Supervisors
Dr. Claudio Fiorino
Dr. Roberta Castriconi

Examiners
Prof. Stefania Pallotta
Dr. Lorenzo Placidi

Postgraduate Thesis of
Pier Giorgio Esposito
Matr.S62562

Academic Year 2019/2020

To all the VIP in my family

"Ogni lasciata è persa"
Parole di mio nonno e di Orazio prima di lui

Abstract

The aim of the present work is to propose an originally developed Knowledge-Based approach for large scale implementation of automatic plan optimization for whole breast radiotherapy delivered, with tangential fields (TF) arrangement. The commercially available tool RapidPlan® (RP) from Varian Medical System has been used to generate DVH estimation models starting from available cohorts of TF plans manually optimized by using wedged or intensity modulated (Field-in-Field) beams. The same concept was finally extended to an inverse planned technique in use at our Institute, delivered with TomoTherapy® (TomoDirect™).

(a) Development and validation of ViTAT

RP may be applied only to inverse-planned modalities. For this reason, we originally developed and implemented a rotational technique, named Virtual Tangential-fields Arc Therapy (ViTAT), aiming to mimic the dose distribution resulting from TF plans with the explicit intent to make TF plan optimization fully automatic. ViTAT plans consist of four partially blocked arcs where delivery is only taking place in the first and last 20° of rotation of the arcs. The start and stop angles of the arcs were assessed by studying the population of the beams position for the TF plans. A virtual bolus was used during optimization to take into account intra and inter-fraction deformation and movements: different combinations of thickness and density were considered. The PTV was expanded in the antero-lateral direction by the same value as the bolus thickness. The ViTAT feasibility was tested on 40 patients equally divided between left and right-sided breast. Comparison between ViTAT and clinical TF plans was carried out in terms of dose-volume parameters: $V_{95\%}$, $D_{1\%}$ and dose standard deviation for PTV; mean doses and $D_{2\%}$ for OARs. ViTAT optimal characteristics required the arcs range to be [60°-220°] for the right side and [300°-135°] for the left side. ViTAT mean DVHs over the 20 patients population was very similar to the TF ones. There was an improvement in PTV dose homogeneity (0.1Gy $p<0.05$) without a meaningful change in PTV coverage ($p > 0.05$). Concerning OARs there was a worsening/improvement in the 2-15 Gy / 20-35 Gy respectively for ipsilateral OARs, but no change in the mean doses. Contralateral OARs mean doses were improved alongside with the integral dose to body (0.9 Gy lower $p<0.05$). Deliverability was tested obtaining a mean γ index (3% - 3mm) of 99.5 ± 0.5.

(b) KB-models for tangential fields and full plan automation through ViTAT

Once implemented the technique, two KB models were generated, one for the right case (90 patients) and one for the left case (113 patients). As mentioned, regression models were generated using the RP tool for ipsilateral OARs (lung and heart for the left case) and the contralateral breast. Outliers were studied and excluded if found to be associated with suboptimal plans. Templates for automatic plan optimization based on the resulting KB models were generated. The position and priorities of objectives were fine-tuned by optimizing

them iteratively over a set of 5 patients for the right case and 5 for the left case. KB fully-automatic ViTAT (KB-ViTAT) plans were realized for 30 patients for each side and compared in terms of dose volume parameters. 10 out of 90 (Right) and 18 out of 103 (Left) patients were excluded for at least one structure from the model, being considered outliers. KB-VITAT automatic plans showed similar results with respect to clinical TF plans in terms of PTV coverage and OARs mean dose and shape of DVH curves with a slight (statistically significant) improvement in PTV homogeneity and body integral dose. 1 out of 30 and 7 out of 30 plans were considered not acceptable and needed a refinement after the automatic optimization. Interestingly just shifting the start and stop angles of the arcs by 5° and running again the optimization, was enough to obtain an acceptable plan in accordance with the dose distribution of the TF one.

(c) KB for TomoDirect™ and full plan optimization in the TomoTherapy® environment

A TD specific model for left-sided breast cancer patients (69) was generated in Varian TPS using RP. A template was fine-tuned and optimized iteratively on a 5 patient set choosing the optimal structure importance priorities and objective position. The template is automatically sent from the Varian system to TomoTherapy® TPS via ESAPI. An internal validation on 30 patients and an external one on 10 patients was carried out to test the performances of the model. 9 out of 69 patients were excluded for at least one structure from the KB-TD model for the left-sided breast. In the internal validation PTV coverage was improved (1% $p<0.05$) alongside with $D_{1\%}$ (0.4 Gy) and homogeneity (0.09 Gy). Ipsilateral mean dose was improved ($p<0.05$) with the automatic approach by 0.1Gy/0.2Gy for ipsilateral lung/heart respectively. For 4 plans out of 30 it has been necessary to add beams to a total of four segments in order to achieve an acceptable plan. In the external validation the general behavior was replicated even though the differences were not significant ($p > 0.05$) anymore. Time necessary to deliver KB-TD plans is 8 ± 1 min to be compared with 6 ± 1 min and 8 ± 2 min that are the time necessary to deliver 5 cm field-width-plans or 2.5 cm ones, respectively.

In conclusion, we proposed an approach for large-scale automatic planning in a Varian environment. It is currently used in our clinical practice (40 patients were treated: four ones needed shift of the arc angles and four ones needed manual refinement), taking only 12 ± 2 min to generate an optimal plan, comparable to TF manually optimized plans. The same approach was followed to automate planning for left-sided breast cancer in a different environment: the KB-TD model is soon to be clinically implemented.

CONTENTS

Introduction

In the female population, breast cancer is the most common form of cancer. The WHO Report on Cancer [1] estimates that in 2018 the breast incident cases were 2 088 849 globally, corresponding to 24.2% of the total cancer cases among women. A well assessed and effective therapeutic option is the breast-conserving surgery, followed by whole breast radiotherapy to sterilize the site. [2, 3] Treatments are following a hypofractionated protocol delivering 38-40 Gy in 15-16 fractions or the standard 50 Gy in 25 fractions. Techniques are evolving leaning toward more personalized approaches to reduce the treated volume with the partial breast irradiation or delivering a higher dose to a specific site (Simultaneous Integrated boost) or to include nodal regions in patients at higher risk of regional and/or distant relapses [4–7]. Despite that, whole breast irradiation is still one of the most used breast cancer treatments.

Different techniques are applied to achieve whole breast irradiation. The majority of institutes are using tangential fields (TF) arrangements delivered with 3-Dimensional Conformal RadioTherapy (3DCRT) using physical or dynamic wedges or with Intensity Modulated RadioTherapy (IMRT), delivered mostly using few segments per beam (the so called Field-InField (FIF) approach). Optimization is often a manual process that takes time and planner's expertise [8–11]. Volumetric Modulated Arc Therapy (VMAT) is an inverse-planned rotational technique that shows optimal performances in terms of Planning Target Volume (PTV) dose conformity, associated with a better sparing of Organs At Risk (OARs) in the high-intermediate range of doses, especially in presence of particularly concave PTV [12, 13]. Concerning the low dose, rotational techniques lead unavoidably to an increase of the dose bath, even far from PTV; the clinical meaning of this dose spread (especially to heart, lungs and contralateral breast) is controversial, due to the lack of knowledge with respect to the potential increase of late cardiac mortality and secondary tumors [14, 15]. Instead, TF geometry arrangement conserves the possibility to limit the low dose spread and for this reason, it is most likely going to be still proficiently used for a long time.

It has to be considered that manual, and to a lower extent also inverse planned, optimization is highly time consuming and planner dependent [16]. Standardizing the radiotherapy treatment is a key factor to guarantee a high quality plan to all patients, independently from planner's skills and time availability [17, 18]. Automatic planning approaches could help reaching an optimal plan, reducing the time needed to obtain it and limiting the intra-operator variability [19–22]. There are many approaches to auto-planning that were largely investigated for various clinical

applications, breast cancer included [23–27]

However, automatic optimization of TF plans for whole breast irradiation is not an easy task. Inter-patient variability influences the choice of the optimal field position. A sub optimal beam geometry is correlated to suboptimal plan and consequently a higher dose could be released to OARs or PTV coverage could be worsened. Some in-house solutions were proposed but their application to a larger scale is intrinsically difficult [16, 26, 28]. Knowledge-Based (KB) approach is suitable to implement an automatic optimization for TF plans, since there is a large availability of past treated patients.This largely available information can be modeled and used to generate a prediction on new patients. A commercially available system that allows the generation of a KB prediction model is the RapidPlan® tool from Varian Medical System, Inc. It works as a Dose-Volume Histogram (DVH) estimation algorithm, allowing to predict expected DVH for new patients and this information may be translated into an individualized template for automatic plan optimization. It was tested and applied to many clinical scenarios, including VMAT breast [23, 29, 30]. There are no clinical examples for TF whole breast irradiation, most likely due to the configuration of the system that was implemented for inverse-planning optimization. There is then the need to implement an inverse-planned TF irradiation methodology.

Moreover, although the RapidPlan® tool is implemented for the Varian environment, there are application examples on machines and TPS from different systems, such as the TomoTherapy® from Accuray, Inc. [31, 32], but no clinical examples were reported for the breast site.

Within a project for large-scale implementation of automatic optimization (MIKAPOCo, Multi-Institutional Knowledge-based Approach to Plan Optimization for the Community) the following aims were selected:

1. To explore the possibility to mimic the dose distribution and performances of TF irradiation through a partially blocked multi-arc approach using the “avoidance sector” option of a rotational technique optimized via RapidArc® (Varian Medical System, Inc.). VMAT technique with partially blocked arcs was investigated by many groups to reduce the low-dose spread associated with arc techniques [33–36]. Our approach is different from the previous ones because we aim to mimic exactly TF dose performances. We called the implemented technique Virtual Tangential-fields Arc Therapy (ViTAT).

2. To implement KB-models for right and left-sided breast cancer treatment, based on past TF plans. These models are used to drive the inverse-planned ViTAT technique and we aim to replace TF manual optimization with the automatic KB-ViTAT approach.

3. To test the performances of the KB-ViTAT models in predicting the correct DVHs for patients treated on a different machine and system environment, the TomoTherapy® in TomoDirect™ modality.

4. To generate a model for the left-sided breast cancer patients specific for the TomoTherapy® machine in order to automate the manual inverse planning of the TomoDirect™ modality.

The thesis is structured as follows. Chapter 1 contains an introduction on automation in radiotherapy focusing on the approaches that allow automatic optimization and showing the main characteristics of the commercially available system RapidPlan®. In Chapter 2 an overview on guidelines and breast treatment modalities is presented, focusing on the protocols followed in our institute. Chapter 3 contains the materials and methods of the whole work, while Chapter 4 shows the results that are discussed in Chapter 5.

This project was entirely developed and carried out at IRCCS Ospedale San Raffaele in Milan, Italy. Data collection and data analysis took place along the three years formation period for my Postgraduate School of Medical Physics at University of Milan, Italy.

CHAPTER 1

AUTOMATION IN PLANNING OPTIMIZATION

In this chapter, automation in Radiotherapy (RT) will be discussed in terms of modalities and techniques, showing the currently available methods and tools to take advantage of a prediction model and how to evaluate its performances, focusing on a specific commercially available software.

Modern RT has been the field for many technological advances in both machine and techniques capabilities. The treatment sophistication becomes higher and higher especially with the advent of Image-Guided RadioTherapy (IGRT) and Intensity Modulated RadioTherapy (IMRT) and its evolution to rotational IMRT, the so called Volumetric Intensity Modulated Arc Therapy (VMAT). The advent of complex machines and techniques modality in modern RT allowed to reach higher tumor conformity and normal tissue sparing around the target, even when the geometry is not favorable.

Reaching a higher conformity helped developing new treatment techniques such as the Simultaneous Integrated Boost (SIB), where higher doses are delivered in selected portions of the PTV, aiming to increase the Tumor Control Probability keeping the same or lower risk of side effects for patients.

This high-level of complexity proceeds together with software incrementing capabilities that are nowadays at their highest level, allowing the treatment in a much faster way than before. Artificial Intelligence and automation are the key words of this new era where software is helping users to provide the same (or improved) treatment quality to the patients with efficient, consistent and cost-effective solutions.

1.1 Radiotherapy and automation

A typical IMRT treatment starts from a Computed Tomography (CT) scan where Clinical Target Volume (CTV), Planning Target Volume (PTV) and Organs At Risk (OAR) are normally manually delineated by clinicians. Different clinicians inevitably draw different ROI depending on new imaging technologies, accessibility to other imaging modalities, followed protocols, experience and time availability. [17, 18]

After delineation, planners create control structures (also called ghost or shell) Regions Of Interest (ROI), that are not associated with any precise anatomical area, but are very useful during optimization. These structures are intrinsically different between different operators. Protocols may be introduced to reduce variability, but every user modifies the shells depending on their optimization strategy and on their experience.

Another crucial step is the definition of plan geometry. Especially when dealing with IMRT plans, it is really important to select the "right" angles position and dimension for the treatment, focusing on the best OARs sparing and minimization of dose-bath to normal tissue and whole body. Beam angles definition is very critical if the planner is not experienced enough and depending on the treated district the differences may be not negligible.

Once the setup of the plan is defined, the starting objectives of the template have to be determined. This step is relevant when dealing with inverse planning optimization, where the final IMRT fluences of the fields/arcs critically depend on this setting and on the changes required during the optimization loop. This is another personalization issue, as users may work from different starting points trying to converge, more or less efficiently, to the optimal solution. In fact, templates are often stored on the machine to be used as a starting point for optimization, but users may decide to save new personalized protocol templates making the plan optimization still highly operator dependent.

Finally, there is the optimization loop; depending on the modality of treatment delivery, it can either be a manual loop or an automatic loop (inverse planning optimization with cost function). Here at every loop the user or the software is asked whether the plan is clinically acceptable and optimal dose distribution has been reached. If this is not the case, there is an adjustment of the objectives or a modification of the conformation of the Multi-Leaf Collimator (MLC) or delivery angles until the criteria for acceptability are met. Although the acceptability criteria are objectively given, the risk to stop the loop before the optimal plan has been found, is high, especially for inexperienced planners.

The ideal workflow assumes the possibility to automate some or all of the steps of this process. Automation in contouring is also an emerging field; many recent experiences with automatic systems are showing very good agreement between radiation oncologists and software contouring, similar to the intra-operator differences [18, 38].

In this environment the physicist's job is to create an optimal plan and automation is shining the most when applied to planning. This application is increasingly gaining more interest in the

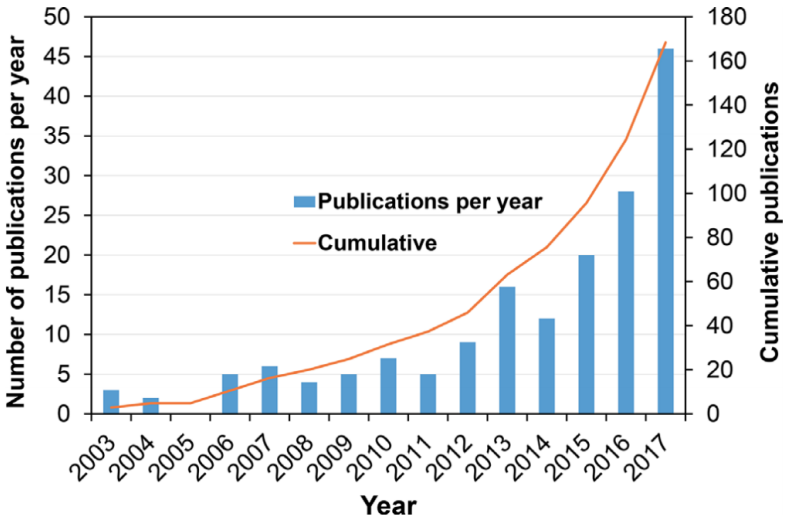

FIGURE 1.1. Image from Hussein et al. [37]. Original caption: "Trend showing the number of peer-reviewed publications on innovations in automated planning software per year, and the cumulative number of publications. The graph shows a significant increase from 2011".

last ten years as shown in Figure 1.1.

When talking about automated planning we expect that for each patient the computer is able to generate fully automatically the treatment plan. It is a "push-button system". Plan is supposed to have the highest clinical quality and it should be also Pareto-optimal.

Alternatively, it is possible to create an automatic plan that is successively manually fine-tuned by the planner. The automatic plan is used as a starting point to reach a better and improved final plan that should be obtained in an easier way than the fully manual optimization.

According to Hussein et al. [37] automatic planning systems may be divided in three categories: the protocol-based automatic iterative optimization, the ones based on multi-criteria (also called multi-objective) optimization; the knowledge-based planning optimization.

1.1.1 Protocol-based automatic iterative optimization (PB-AIO)

PB-AIO employs a template that contains some fixed constraints that need to be satisfied, called "hard constraint" and others that have a lower importance.

The system starts from a template defined by the user. Once the constraints are met the objectives with the higher priority become hard constraints and the system iteratively adjusts the objectives and constraints, lowering the DVH of all the structures, as long as the hard constraints remain unviolated. The template needs to be carefully set, properly introducing the priorities of all the objectives resulting in final plans satisfying the clinical expectancies of the physicians.

Many groups implemented this approach on their own, creating scripts that are able to mimic

human behavior while planning or, more rarely, artificial intelligence that uses fuzzy logic theory to describe an expert planner trial-and-error process solving a problem. This logic is translated into binary programming “if statements”. [19, 39–41]

There are also some commercially available systems that use this approach. An example is "Pinnacle" embedded in the Philips Treatment Planning System (TPS) (Philips Radiation Oncology System, Fitchburg, WI). The user creates a template with the prescription and the dose constraints to OARs giving also all the priorities for all considered structures. The system automatically creates all the overlapping structures, shells, rings and ghosts structures necessary to planning and uses them to optimize the dose distribution in terms of dose-fall and dose bath to body. The iteration lasts for five loops before reaching the final solution presented to the user. [40, 42]. In literature there are many examples of PB-AIO in various clinical applications: head and neck, prostate, rectum and esophagus. [43–47]

1.1.2 Multi-criteria optimization (MCO)

The multi-criteria (or multi-objective) optimization circles around the concept of Pareto optimal solutions. In this kind of plan it is not possible to improve any criteria without losing something on the other ones. [20, 21, 37]

There are two different approaches to MCO the “a priori” and the “a posteriori” that require slightly different user interaction.

A posteriori

In the a posteriori approach the system generates a multiple set of Pareto optimal plans. The optimizer creates various solutions that stay all on the so-called Pareto front, where it is not possible to modify a certain criteria without influencing another one.

The user is presented with all the plans and it is possible to select which solution is clinically better for the patient. Selecting a different solution would mean to select an improvement in some criteria, with a worsening in some others. Plans on the Pareto front are not clinically optimal, but the clinically optimal plan is on the Pareto front. [37]

Mathematically speaking, there are an infinite number of plans on the Pareto front. The computing capacity of the hardware is the limiting factor of the number of possible solutions. It has been found that an estimate of the optimal number of solutions to be shown in the solution is equal to the number of objectives plus one. Moreover the final solution is user dependent, because it is related to the choice of the plan. It has to be noticed that all the solutions are obtained fully automatically.

There are two main commercially available software that allow a posteriori MCO that are the RayStation TPS and the Varian Eclipse TPS. There are clinical applications reported for prostate cancer, head and neck, brain and lung. [48–51]

A priori

In this case the system gives as a result just one Pareto optimal plan. The selection of this plan is not in the hands of the user, to be made at the end of the process. In this case there is a template of hard constraints that have to be fulfilled and a "wish list" of objectives associated with a certain priority. The optimizer finds solutions that respect all the hard constraints and it tries to find the optimal clinical solution on the Pareto front as a trade-off between the objectives of the wish list. Iteratively the wish list is improved until the best clinical plan quality is reached. It is intrinsic in the optimization modality that this technique guarantees always the best quality achievable and the overall planning quality is improved. On the other hand, the selected solution critically depends on the initial definition of selection criteria.

The Erasmus-iCycle from Erasmus MC Cancer Institute, follows this approach and has been among the first to be clinically applied in many sites such as head and neck, prostate cancer, lung cancer [52–56]. Recently Elekta (Elekta AB, Stockholm, Sweden) has developed and commercialized a new auto-planning tool [57, 58] using the concepts of "a priori" MCO and wish-list, already implemented in Erasmus-iCycle.

1.1.3 Knowledge-based planning

Knowledge-Based (KB) planning is based on a different approach. While in the auto-plan approaches the previous clinical plans are used as a starting point to set templates or wish lists of objectives, in this case the previous knowledge is used directly to predict what would happen in a new case. This information can be used to obtain a new plan, fully automatically optimized or to set a starting plan for further modification and fine tuning.

According to Ge and Wu [59], methods for KB planning may be divided in two categories: case and atlas-based methods on one hand and statistical modeling and machine learning methods on the other.

(a) Case and atlas-based methods

This is the most intuitive system of KB approaches. The prediction on a new patient is based on similar cases found in the set of prior clinical plans [60, 61]. Similarity is established either using a direct approach using image features, structures or clinical variables, or using an indirect approach. In the latter case a model based on features is generated with the aim to predict some dose parameters and they are used to find similar cases.

(b) Statistical modeling and machine learning methods

In this category a statistical model is generated using different methods: regression models, logistic or Poissonian regression, curve fitting, artificial neural networks, support vector machine and clustering. The idea is to find a descriptive index for the anatomical characteristics of my sample of patients. The system will create a model that needs to be trained in order to

associate this index to a certain level of dose received by patients. KB model training requires high quality plans, because the quality of the output plan for the new patient is equal or just slightly better than the training ones. The most recently developed KB approach has been implemented in the Raystation® 8B*. A machine learning algorithm is used to learn from prior plans. It predicts the 3D dose distribution for new patients using a dose mimicking optimization, generating a deliverable treatment plan. [62]

In general the most common applications of KB planning concern the guidance of Dose-Volume Histograms (DVH) that will allow the creation of a template to be used in the optimization process. A KB model needs to be generated for each clinical scenario (a given technique and particular set of patients receiving similar treatments). The export of a model to other centers or if it is wanted to change the treatment modality from IMRT with fixed fields to VMAT, is in principles not an easy task and a series of parameter have to be considered when dealing with different modalities. Nonetheless, there are studies that used TomoHelical™ data to create a model later applied on different machines for VMAT planning. [32]

Clinical applications of KB automation planning have been implemented for many cancer treatments sites, such as breast cancer, cervical cancer, lung, rectum and prostate cancer. [25, 31, 63–66]

Moreover it is also possible to use a commercial system (the RapidPlan™ tool from Varian) to create models delivered using different brand TPS and machines, exporting the predicted DVH to the new TPS. [32, 67]

The most established commercially available system using the KB approach is RapidPlan™ (RP) from Varian Medical Systems, Palo Alto, CI. [68] RapidPlan™ tool is part of the second aforementioned category: statistical modeling methods. This is the system used to realize this work and to create KB models to obtain a prediction on the DVH of new patients starting from information of clinical manually optimized plans.

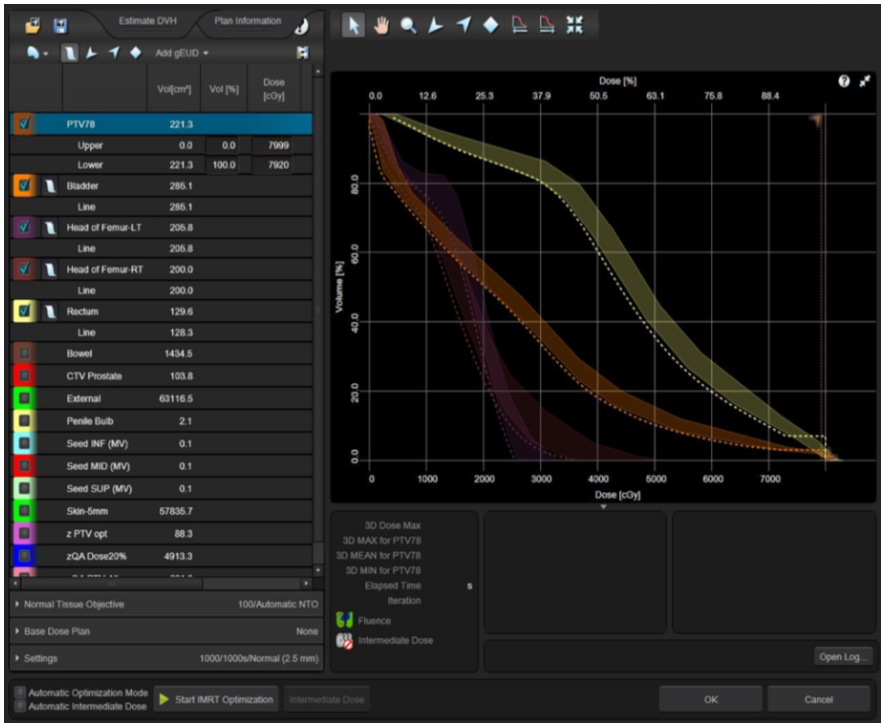

FIGURE 1.2. Image modified from [68]. Graph presented by the RapidPlan™ tool to show DVH-Estimate (region band). When selecting objectives for the template, the system selects them using the dotted line, slightly below the low band.

1.2 KB Commercial system RapidPlan™

As aforementioned RapidPlan™ is a commercial system implemented in the Eclipse TPS of Varian Medical Systems, Inc. since version 13.5 of Eclipse TPS. [68, 69]

It allows KB automatic planning using previous clinical plans. In particular it uses information about dose and patient anatomy. It gives as a result DVH-estimates (DVHE) so as to have knowledge of the possible outcome of the dose distribution in a new patient.

A DVH estimation model created with this software presents the DVHE as a range (Fig. 1.2), showing where the DVH could most likely land for a new patient.

KB models can be generated for different techniques, both IMRT and VMAT. The technique has to be inverse optimized using a template. This system, indeed, allows automation creating a template that is then used during optimization. The template has to be defined when generating the model and it requires fine tuning in order to obtain the most out of the prediction model.

1.2.1 DVH estimates algorithm

When generating a DVH-estimation model it is very important to have in mind the kind of model one wants to create. It is possible to create a model that is technique specific or it could be applied

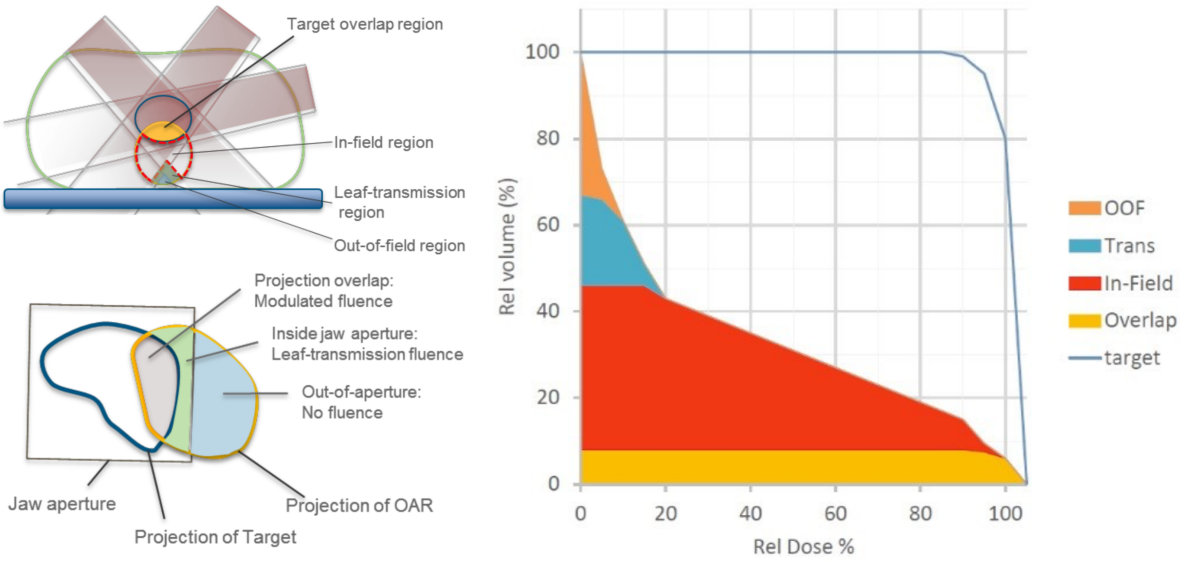

FIGURE 1.3. Images modified from [68, 70]. Sub-volume OARs partitioning for DVH estimation in RP tool from Varian. Sub-volumes are singularly considered and they are combined together considering the relative volume as a weighting factor in order to obtain the final DVHE. Top left: transversal view for a generic IMRT plan. Bottom left: BEV for a field in a generic IMRT plan. Right: DVH partition based on the dose received by the four sub-volumes.

to a variety of protocols. This decision is reflecting on the types of plans that are going to be selected for model training.

Once the patients have been selected the system extracts from each one of them the anatomical information of selected contours and the dose distribution of the associated plans. The model is site specific and the OAR structures used have to be preselected. A DVHE model generates a separate estimate for each selected OAR structure. Every "structure model" is independent from the other ones and any possible correlation between OARs is not considered.

OARs and target structures are considered differently inside the model. The geometrical correlation between the target structure and OARs is used to find the DVHEs. To do so, the system partitions the OAR volume in four different sub-volumes: Out-Of-Field (OOF), Leaf-Transmission, In-Field and Target Overlap regions. This partition is generated from the Beam-Eye Views (BEV) from all the directions of the beams (Figure 1.3). RP considers that in the OOF region only scattered dose is present and there is no direct exposure of this region by any field. In the Leaf-Transmission region, there is no direct exposure as well, but the transmitted dose through the MLC is considered. Optimization will not affect this amount of dose received by this region, only the MU delivered by the field are. In the In-field region, the dose exposure varies depending on the optimization process. The contribution of this region affects the DVHE the most. In the Target Overlap, the dose exposure is comparable to the one delivered to the target and so optimization

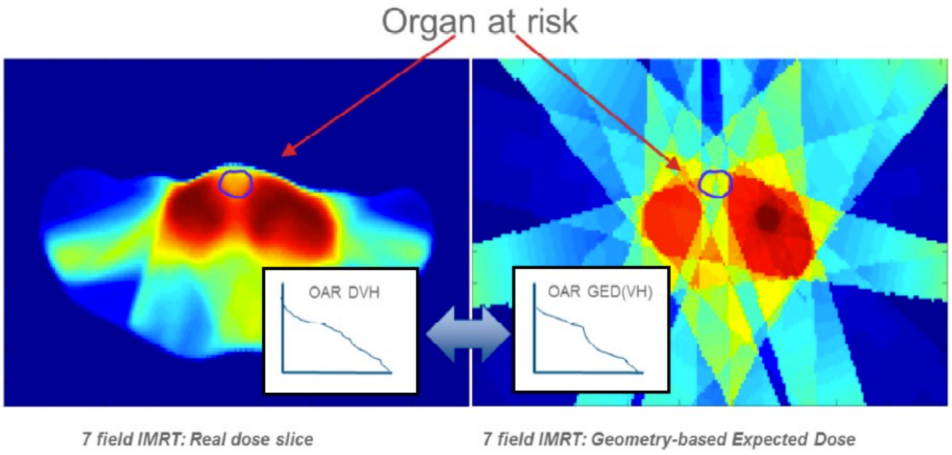

FIGURE 1.4. Image from [70]. Original caption: "Example of GED field construction for a 7-field IMRT plan: real dose distribution (on the left) and GED configuration (on the right). Once the GED field has been constructed, the geometrical position of individual OARs is evaluated by calculating a GED cumulative-volume-histogram (GEDVH) inside the OAR volume."

will only slightly affect the DVHE output.

Every sub-volume is evaluated separately during the training phase and it is weighted by the corresponding volume before combining every part. All OARs evaluations concern the relative position with respect to target structures. RP can handle a maximum number of three targets at the same time.

Two model approaches are used to predict the DVHE. A simple model approach is used for OOF, Leaf-Transmission and Target Overlap regions where the dose exposure is based on DVHs variation in the training set. For each aforementioned region, a model is generated using the simple approach. It is required that at least two instances of each sub-volume are not null in the training set. If that happens the system uses a default model where the OOF region is considered to have zero dose exposure. The leaf transmission and the target overlap are considered to be a constant value equal to the 5% of the dose and to the target prescription dose respectively.

The second approach, less straight-forward, uses a regression model for the DVH estimation. The In-field sub-volume dose exposure is calculated using this approach. There are three step to be followed: geometry evaluation, dose parameters estimation and DVHE construction.

The geometry evaluation is based on the Geometry-based Expected Dose (GED). This means that the distance between sub-volume and target is converted into dose units. Using these metrics, the system is able to take the field geometry or the presence of multiple targets into account.

Once GED is generated, it is possible to calculate the Geometry-based Expected DVH (GEDVH). The system extracts the DVH information of patients and tries to correlate them with the GEDVH (Figure 1.4).

In the training phase, a Principal Component Analysis (PCA) is performed to parametrize

both the DVH and GEDVH curves. Moreover, other parameters that are registered are OAR absolute, overlap and relative out-of-field volume and absolute target volume.

PCA consists in using specific curves, referred to as Principal Components (PCs), that can be linearly combined together with the training mean DVH set to describe DVHs or GEDVHs of any patient. The number of PCs necessary may vary depending on the population variability of anatomy and DVHs. In general two/three principal components are sufficient to express the DVH variability. The scores associated with every PCs are recorded.

For a certain patient the PCs scores are calculated. The related DVH can be generated linearly combining the mean DVH and PCs using the associated scores. A regression model is then trained using these parameters, calculated for the whole initial set of patients.

The lower and upper band of the DVHE are given spanning the interval around the DVH obtained using the standard error of the regression.

1.2.2 Optimization constraints and templates

When the regression model is applied on a new patient the following step are performed (Figure 1.5):

- The PCA analysis on the geometrical position of OARs allows to find the PC scores for GEDVH.
- The regression model is used to obtain the predicted DVH PC scores and the mean predicted DVH is found for the in-field sub-volume.
- The other sub-volume partitions are considered adding the corresponding mean value of the training set.

The model generates the most probable DVH and the lower and higher band of the DVHE are found using the standard error of the regression.

A template can be created selecting objectives for defined dose or volume parameters. The corresponding volume and dose values, respectively, are selected slightly below the lower band, as shown in Figure 1.2. The kinds and the number of objectives are decided when setting the DVHE model.

The different constraints that may be set will vary the behavior of the optimizer. There are hard constraints where the model is not used and the dose and volume parameters are set by the user for every patients; upper constraints where it is possible to generate the volume value or the dose value; it is possible to use a gEUD metric, where it is necessary to set the corresponding "a" parameter and it is also possible to set a line objective. These constraints are the same that are available in the normal optimizer tool of Eclipse TPS.

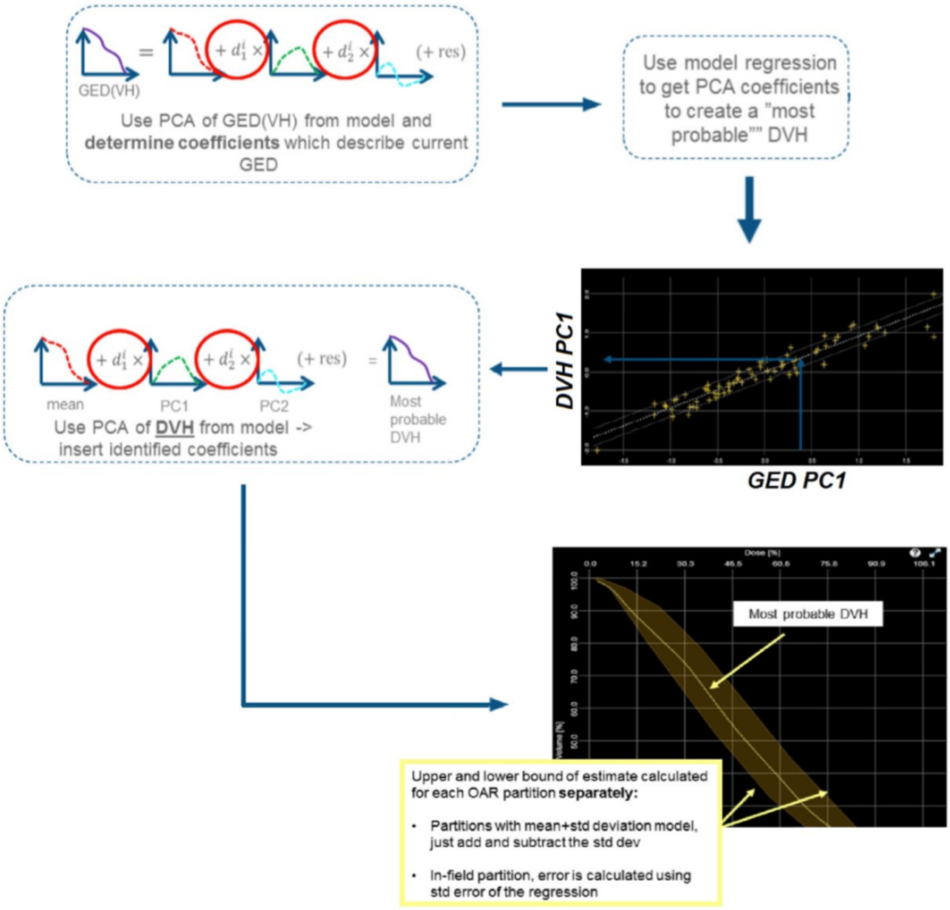

FIGURE 1.5. Image from [70]. Original caption: "For a new patient: the GED-PCs are calculated and the GEDVH for the in-field partitions of OAR is retrieved from the model; the regression model is used to determine the DVH-PC and used to obtain the most probable DVH. The standard deviation of the training set is added and subtracted from the most probable DVH for each partition regions".

The target DVHE depends only on the prescription dose and it is compared to what was used in the training set. The DVHE of the OARs are rescaled considering the new prescription dose the 100% value.

A minimum number of 20 plans are required to generate a prediction model, but in literature it is suggested to avoid training sets with less than 30 patients. [71, 72]

1.2.3 Validating a prediction model

A crucial part of the generation of a new model is the verification of the performances of the model in predicting accurate DVHs. The model configuration process has to follow some steps that will improve the robustness of the outcome. When selecting the patients for the training set it is necessary to use high quality plans and carefully consider outliers to be withdrawn.

Outliers removal can significantly improve the performances of the model. In general, there are two kinds of outliers, the dosimetric and the anatomical ones.

The first category, dosimetric outliers, are related to patients that have been treated with an acceptable, but suboptimal plan. Keeping these plans inside a model would spoil the model performance. It is then necessary to eliminate all the suboptimal plans so that only high quality plans are used for the regression model.

The latter category, anatomical outliers, refers to patients that are characterized by some particular geometry and the dose distribution could differ from the expected trend. This kind of patients could be considered to be retained in the model since they are representing a scarcely present, but still possible geometry and one could benefit from their presence in the model.

Definition of the outlier and statistical study of the model could be performed using the Varian Model Analytic platform or directly the tools that are available inside the RP environment.

Once the model is configured, it is necessary to test its performances. An internal validation comparing the predictions with respect to the clinical DVH for patients inside the training set may certainly show the performances of a model, but an external validation is preferable in order to observe how the model behaves on new patients geometry.

An important step in the configuration process concerns the template definition. The number, the priorities and kind of objectives have to be tuned to obtain the better results from the prediction model. [23, 73, 74]

The best way to verify and validate a model is to compare automatic and recent manual plans, optimized by experts in the absence of time pressure on external patients. It could also be useful to consider treatment time and deliverability.

Moreover it may be interesting to test the exportability of models for other techniques or for other centers, considering the difference in the internal protocols. Harmonizing models created in different institutes could improve their interchangeability. The Multi-Institutional Knowledge-based Planning Optimization for the Community (MIKAPOCo[75]) project is now trying to work on this matter, comparing models generated in different Italian centers, for different sites of treatment. One of the aims of this project is to create a benchmark so that a third party could compare their plan quality against the national standard.

CHAPTER 2

ISSUES IN MODERN RADIOTHERAPY FOR BREAST CANCER

In this chapter the reader's attention will be drawn firstly on the clinical context of available techniques for breast cancer treatments and secondly concerning specifically the whole breast irradiation techniques. Successively, procedures used in our institute will be discussed.

2.1 The current clinical context

Breast cancer is most commonly diagnosed thanks to mammography screening, which allows to detect and treat early-stage tumors. [76] These kinds of tumors are often treated with whole breast radiotherapy after breast-conserving surgery. [2, 3, 9]

2.1.1 Volumes, dose and fractionation: AIRO guidelines

According to AIRO guidelines [77] the breast has to be irradiated as a whole, up to 0.5 cm below the surface and avoiding the thoracic muscles. The skin is irradiated only if there is tumor infiltration in the superficial tissues.

AIRO guidelines propose various prescription and fractionation considering 5 fractions per week. On one hand the conventional fractionation considers 50 Gy in 25 fractions (2 Gy/fr) or 50.4 Gy in 28 fractions (1.8 Gy/fr). On the other hand, considering a value for the α/β ratio equal to 4 Gy, a hypofractionated protocol could be applied delivering 40 Gy in 15 fractions (2.7 Gy/fr) or 42.5 Gy in 16 fractions (2.7 Gy/fr).

AIRO compares the two fractionation protocols: in terms of clinical outcome hypofractionation reduces acute toxicities (radiodermatitis, edema, pain) keeping the same local control and aesthetic results; in terms of hospital efficiency there is a reduction in the total treatment

duration, better optimizing the resources of the institute. Hypofractionation is now consolidated in early stage breast cancer patients. Heart mean dose and $V_{40\text{Gy}}$ benefits from hypofractionation, considering a value of the α/β ratio higher than 1.5 Gy. [78]

In some cases, it is possible to boost the dose to the surgical bed (total of 60 Gy for conventional fractionation). The boost may be delivered in a sequential or concurrent way: the former consists in delivering two distinct plans sequentially, while the latter requires the generation of a plan with a well fitted dose distribution gradient around the boost and PTV volumes (Simultaneous Integrated Boost - SIB).

The boost is normally avoided for low-risk patients with the aim to reduce aesthetic results, quality of life and costs, while it remains a necessity for higher-risk patients. There are indication on how to detect a high-risk patient, depending on her clinical situations: young women (less than 40 years old), positive histology to surgical margins, positive lymph nodes, negative hormonal receptors, extensive intra-ductal carcinoma and/or iper-expressed HER2[1].

2.1.2 Intra and inter-fraction uncertainties: margins and IGRT

There are various external radiotherapy breast treatment options: 3DCRT, FIF, IMRT, VMAT and TomoTherapy®. Intra and inter-fraction motion reduction for all these techniques is fundamental to ensure accurate treatment localization for the PTV.

There are different approaches to reduce intra and inter-fraction motion that include set-up errors, patient movements and breathing motion: Image-Guide Radiation Therapy, immobilizers and breath hold techniques. One of the most used modalities to limit breathing motion is the Deep Inspiration Breath Hold (DIBH) technique with or without the use of Active Breathing Coordinator (ABC). ABC helps the patient to hold the breath in a steady and repeatable way. In general DIBH is used to regularize or limit the breathing motion during treatment. Generally the breathing motion is of small entity and DIBH is used mostly because it is helpful to create distance between heart and PTV, especially for the left-sided breast. [79]

The patient is asked to be steady for the whole duration of the therapy, but sometimes patients modify their initial position due to discomfort or relaxation. Immobilizers of legs and torso reduce the residual motion of the patient. [80]

Before IGRT, patients were positioned only using lasers and skin marks. With the advent of IGRT, it was possible to use imaging to more precisely position patients before treatment, reducing uncertainties due to set-up. The standard imaging verification technique is the Electronic Portal Imaging Device (EPID) acquiring two-dimensional mega voltage images. These images are compared to Digitally Reconstructed Radiography (DRR) generated in TPS from planning CT for the lateral and medial tangential beams. Cone Beam Computed Tomography (CBCT) or Mega

[1]HER2 (Human Epidermal growth factor Receptor 2) is a protein that promotes the growth of cancer cells. If this protein is extensively expressed then the tumor tends to be more aggressive.

Voltage Computed Tomography (MVCT) could also be acquired before treatment and compared to planning CT for positioning.

Depending on immobilization, set-up protocol and eventual breathing management, some margins have been used to expand the Clinical Target Volume (CTV) to Planning Target Volume (PTV).

Harris et al. [81] show that using only surface markers, set-up errors range from 1 to 30 mm. The PTV expansion margin normally used before IGRT was 10 mm while IGRT, even if not daily used, reduces the inter and intra-fraction motion to be generally lower than the 5 mm. In some cases there are movements or deformation that could lead to exceeding these margins. As described by Michalski et al. [82], daily IGRT allows to avoid these errors keeping the margin to 5 mm. Lowering the margin is possible but motion has to be limited, for example using breathing hold techniques.

There are some studies suggesting that these margins could be lowered for specific treatment modalities. For example Goddu et al. [83] proposed a margin of 3 mm for TomoHelical treatments.

2.2 Whole breast RT techniques

Different geometries and treatment modalities can be used for whole breast cancer patients. Let us focus on the most consolidated techniques.[84]

Wedged 3DCRT

Delivery takes place with two opposed or quasi-opposed tangential fields. Their position is chosen trying to limit heart and lung overlap from the BEV of the field. The MLC allows shielding of normal tissues, while leaves are left open in air. To ensure the best homogeneity to PTV, wedges are used to account for differences in tissue thickness along the field. Wedges can be physical or dynamic. Dynamic fields allow to reduce the scattered portion of photon from the gantry. If the PTV is large, reaching an adequate coverage could be harder, causing the presence of hotspots within target or normal tissue. It has been demonstrated that 3DCRT improves local control probability [85] but some concerns remain for OAR toxicities, especially for some concave shapes of left-sided breast PTV where a large portion of the heart may receive higher doses. [81, 86]

Manually optimized segments (FIF - IMRT)

Tangential fields arrangement similar to the 3DCRT is used. Instead of using wedges, homogeneous dose distribution is reached using more manually optimized segments whose MLC is manually modified to block hotspot or improve PTV coverage. Segments are positioned at the same angles as the main fields and they are differently weighted. Typically 2 or three additional segments are used per beam. Plans are forward-optimized generating a plan with more, but still limited, degrees of freedom. These kinds of plans are also called Field-In-Field (FIF). FIF has

slightly better performances with respect to 3DCRT reducing hotspots because segments are added to the plan with that specific purpose. [84]

Inversely optimized IMRT

Inverse-planned IMRT uses an optimization algorithm that iteratively modifies the MLC and intensities of fields to generate fluence maps that allow to shape dose distribution. IMRT fields normally range between 2 and 4 beams, arranged tangentially, with few cases using more. It is possible to add a beam perpendicularly to PTV to increase dose conformity to target. Inversely optimized techniques have intrinsically better performances in terms of PTV homogeneity and maximum and mean dose to target. [84]

VMAT

VMAT is a rotational technique delivering dose continuously along an arc. It is an inverse-planning modality where typically MLC and beam intensities are optimized by the algorithm, while the rotational speed is kept constant. VMAT has a high number of degrees of freedom and it is able to better conform dose around the target with respect to the techniques here introduced. On the other hand VMAT increases the spread of lower doses to normal tissues, causing a low-dose bath to lung and hearth. Normally one or two arcs are sufficient to obtain good PTV coverage and dose conformity. [87]

Tomotherapy

Alternatively to conventional linac systems, it is possible to use the Tomotherapy Hi-Art system. It can be used in different modalities the first of which is helical tomotherapy. It is an inversely-planned rotational technique that delivers fan beams rotating the gantry around the patient while the couch simultaneously translates through the bore. The second modality deliverable in tomotherapy is the topotherapy, commercially known as TomoDirect™ . In this case the gantry is positioned at some fixed angles delivering an inverse-planned intensity modulated fan beam while the couch translates through the field. There are various parameters that can affect dose conformity, such as the pitch, modulation factor and field width, but better conformity is usually correlated with higher delivery time. [83, 88]

These techniques generally require the use of only photon beams with energies in the range 6-10 MV with just few cases using up to 18 MV beams. [81, 83–88]

Whole breast irradiation - 40 Gy in 15 fractions		
PTV	$D_{95\%} \geq 38$Gy	
	$D_{5\%} \leq 42$Gy	
	$D_{2\%} \leq 42.8$Gy	
	$D_{1\%} \leq 43.2$Gy	
Ipsilateral Lung	$V_{16\text{Gy}} \leq 15\%(20\%)$	
	$V_{8\text{Gy}} \leq 35\%(40\%)$	
	$V_{4\text{Gy}} \leq 50\%(55\%)$	
Contra. Lung	$V_{4\text{Gy}} \leq 10\%(5\%)$	
Contralateral Breast	$V_{16\text{Gy}} \leq 15\%$	
	$D_{1\%} \leq 2.4\text{Gy}(3.8\text{Gy})$	
Heart	*Left-sided breast*	*Right-sided breast*
	$D_{mean} \leq 2.5\text{Gy}(4\text{Gy})$	$D_{mean} \leq 2.5$Gy
	$V_{16\text{Gy}(20\text{Gy})} \leq 5\%$	$V_{16\text{Gy}(20\text{Gy})} \leq 1\%$
	$V_{8\text{Gy}} \leq 30\%(35\%)$	$V_{8\text{Gy}} \leq 10\%(15\%)$

TABLE 2.1. Optimal constraints in our institute.Inside the parenthesis there are the acceptable ones, parameters should never be higher than these values.

2.2.1 Our institute experience

At our institute, a significant part of the totality of breast cancer patients is treated with whole breast irradiation. They receive 40 Gy in 15 fractions (2.67 Gy/fr), prescribed as mean dose to the PTV. Patients are in a supine position and they keep their arms above the head, to avoid inclusion in the field. A Posiboard™ (CIVCO Inc.) breast immobilizer is used to reduce inter-fraction position variability and guarantee the reproducibility of patient set-up. All patients are positioned using a small inclination angle of 5°.

Mimicking the treatment set-up, a CT scan is performed on patients. The same flat couch and immobilizer tool for therapy is also used during the CT-scan. This scan will be used as planning CT and CTV, PTV and OARs are contoured on it following AIRO national guidelines: CTV is manually contoured slice per slice and cropped with respect to the body with a 5mm margin in order to exclude the skin; PTV is obtained with an isotropic 5mm expansion and it is cropped analogously to the CTV case with 5 mm margin with respect to the surface.

When treated with a volumetric technique, a supplementary 1-1.5 cm expansion of the PTV toward the external part of the body in the anterior-lateral direction is added creating the so-called “Target”. The Target helps in generating a portion of the field delivered outside the body, in the air. This allows to account for margins related to intra-fraction movements due to breathing cycle and to inter-fraction deformation of the breast.

Concerning tangential fields delivered with conventional linac system, MLC leaves of the main fields are opened in the anterior-lateral direction toward air to take into account for intra-

fraction and inter-fraction movements and deformation effects: it is the case, for example, of the breathing motion and the edema side effect. In TomoDirect® leaves are opened towards air by the skin flash tool of the system.

The planning and delivery techniques slightly changed with time. In the last ten years, patients were treated with physically wedged beams. Fields were opposed or quasi-opposed. Plan MLC were manually modified from the Beam Eye View (BEV). Additional optimized segments were used to improve PTV coverage, PTV dose distribution homogeneity and OARs sparing. The angle shift between the prevalent field and the secondary segments is between 5° and 10°.

In 2018 this technique was gradually replaced by the Field-In-Field (FIF) technique [8] without using wedges. In this case the segments use the same position but with a different MLC configuration always with the same aim of PTV coverage and dose homogeneity and OARs sparing. The segments can be merged together to reduce delivery time. For both techniques the isocenter of the field is positioned at the center-of-mass of PTV. Patients were treated using a beam energy of 6 MV with few exceptions where 6 MV and 18 MV beam energies were combined.

A plan is considered acceptable if the constraints in Table 2.1 are respected.

2.2.2 Automation in breast: published experience

Several authors have investigated the possibility to automatize planning for the breast site with the aim to reduce inter-planner variability and optimization time. There are experiences for various treatment modalities and protocols. There are examples of whole-breast IMRT modalities, automated using in house scripting [26, 89, 90] that are able to generate plans in less than 6 minutes. Using the commercially available systems Pinnacle^3 Auto-planning [91], or RapidPlan™ [25] it was possible to reduce mean doses to OARs for IMRT.

There are various automated applications to VMAT whole breast using KB approaches (RapidPlan™ tool) considering SIB irradiation [23] and additional internal mammary lymph node irradiation [24], with reduction of OARs mean doses.

In all these applications, the plan homogeneity was improved obtaining equal or better quality compared to manual plans.

Extending the automation context for whole breast irradiation and aiming to substitute forward-planned TF modalities with an inverse-planned automatable technique, ViTAT was implemented (discussed in next chapter).

CHAPTER 3

MATERIALS AND METHODS

In this chapter the reader's attention will be focused on the materials and methods of the three studies of this work. First a feasibility study of the ViTAT technique will be shown. Then, its application using the commercially available RapidPlan™ tool from Varian Inc. allowed to create a KB-model to automatize the planning process for whole breast irradiation will be discussed; finally the same tool was applied to automatic planning in TomoTherapy®.

3.1 ViTAT feasibility study

The first step is aiming to test the performances of the VMAT technique ViTAT in mimicking the irradiation from tangential fields (TF) for whole breast radiotherapy.

The delivery machine currently being used is the Varian DHX Linac equipped with a 5 mm Millenium MLC; daily image-guidance with CBCT was performed for all patients; plans were optimized using the Varian Eclipse™ TPS system (v.13.6) using the AcurosXB© algorithm for dose calculation.

3.1.1 ViTAT Technique

A few preliminary tests, see later for details, were carried out to assess the feasibility of ViTAT: this technique was defined by the following main characteristics:

1. The delivery takes place using four arcs with 6 MV photon beams. The maximum dose rate used is 600 MU/minute. Irradiation is blocked for the whole arc and it is allowed only in the first 20° and last 20° of rotation. Delivery takes place in a VMAT modality and 20° is the smallest deliverable angle on our machine. This behavior is obtained by setting the proper avoidance sectors in the TPS system while setting the plan. In this way the dose

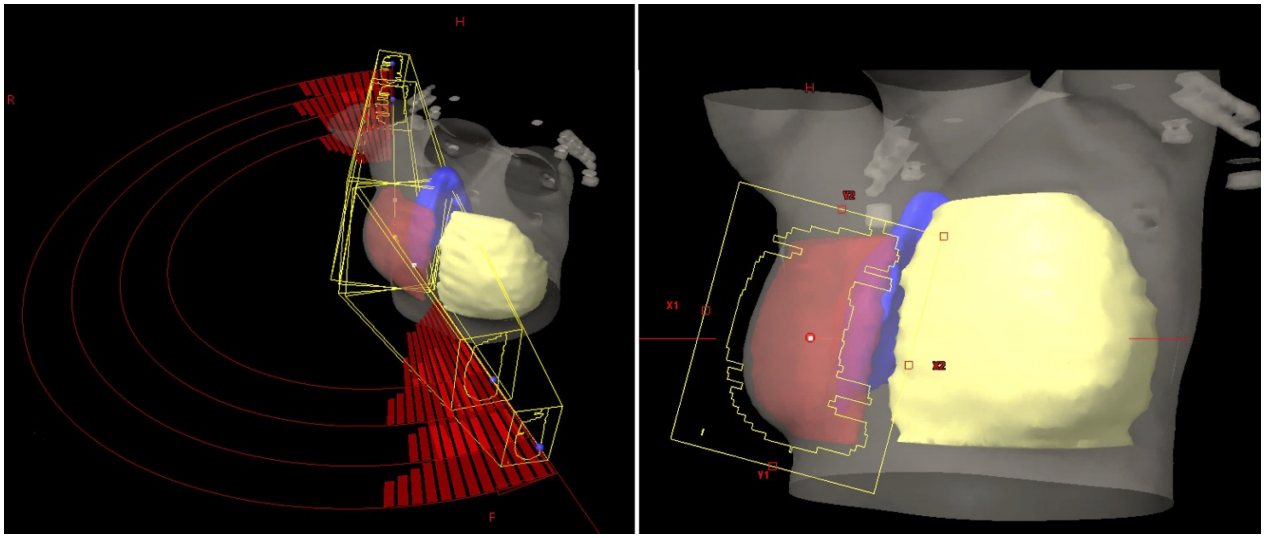

FIGURE 3.1. Image from Esposito et al. [94]. ViTAT technique arc geometry for right-sided breast. The red segments are showing the fluence of the four arcs. The delivery takes place only in the first 20° and the last 20° of the arc (left). BEV of the medial angle start position for one of the arcs (right).

rate in these sectors is a priori set to zero. As before, the field isocenter is set at the center of mass of PTV. Collimator for the 4 arcs is rotated by ±10° and ± 15°. This difference in collimator angle allows to limit the tongue-and-groove effects of MLC.[12, 13]

2. PTV is expanded outside the body in the anterior and external-lateral direction by 1.5 cm, as normally done for VMAT optimization [33]. The created structure is referred to as "Target".

3. A virtual bolus [23, 92, 93] is used during optimization. It is linked to the fields when setting up the plan and it is unlinked before the final dose calculation takes place. (see later) It allows a proper safety margin to take into account for intra and inter-fraction deformation/movements.

4. The arcs start and end angles are set to values obtained from the clinical population data (see later). This ensures with a high probability that among the delivered-(allowed) angles, the optimal ones are included.

5. Fields dimensions are based on the individual patient anatomy. The inverse planning optimization process is carried out using the VMAT optimization module (RapidArc®, RA) in our TPS.

3.1.2 Assessing optimal geometric parameters of the fields

In order to define the optimal start and stop angles of the fields, a preliminary study on the previously available clinical TF experience has been conducted. 80 patients, equally divided between left and right-sided breast cases treated in the last three years have been randomly selected. The prevalent beam angles selected in the corresponding clinical TF plans have been registered for both the medial and distal angles.

The criteria used to select the angle position were slightly different between the right and the left case. Studying the population, modal values were extracted.

Dose delivery happens on a range of 20°. For the right case, the central position of this range is chosen to be equal to the median value found from the population analysis for both the medial and distal angles. The arc will then deliver the dose in the range given by $\pm 10°$ from the modal values obtained.

Concerning the left-sided breast case, the same criteria has been applied to the selection of the distal angle, but the medial angle has been modified in order to assure that there is no overlap between the contralateral breast and the PTV in the corresponding BEV projection. In practice, the medial angle was set to the modal value minus 10°, but if an overlay was present in the BEV view between PTV and contralateral breast, the angle was shifted towards higher values until the distance margin between the two organs was around 0.5 cm- 1.0 cm.

It is worth mentioning that no overlay was observed in BEV view for the right-sided breast cancer patients analyzed in this study, confirming the robustness of our choice.

3.1.3 Assessing the virtual bolus for optimization

A virtual bolus has been used during optimization, as previously mentioned. In order to determine its properties a preliminary study has been conducted on 5 randomly chosen patients. Similar to what was done in investigations found in literature [93], 3 different bolus thicknesses (1.0 cm, 1.5 cm and 2.0 cm) and 2 density values (0 HU and -500 HU) were used during plan optimization. Combining these parameters there were 6 test cases for each patient.

The performances of the boluses were compared in terms of DVH parameters of the PTV after final dose calculation without the bolus. Based on the results, the best solution was identified and applied to all patients for both right and left cases.

3.1.4 ViTAT optimization mimicking clinical TF plans

40 patients equally divided between the right-sided and left-sided breast cases were considered, randomly selected among the population of patients treated in the last three-years. The techniques used to treat these patients are both wedged beams (11 right, 13 left) and FIF (9 right, 7 left). ViTAT plans were generated in order to demonstrate the feasibility of obtaining similar TF plans dose distributions with a VMAT technique and to quantify the differences between

the corresponding dose distributions. The optimization process was conducted in a two-step way method:

- First, concerning OAR dosimetry data, a homemade ESAPI script was used to automatically extract the parameter from the DVHs of the clinical TF plans for every OAR and create a template which could be imported in the RapidArc® module of Eclipse™. PTV objectives were selected according to the clinical criteria explained in the subsection 2.2.1. The starting template used for right and left breast optimization are shown in Table 3.1. These objectives and their priorities have been obtained after optimization and fine-tuning on a few sample patients.
- During optimization the user tried to improve PTV coverage and OARs sparing, trying to limit the low dose bath to lungs, contralateral breast and heart.

For both phases, in order to apply the mentioned criteria of plan optimization, the user optimized the plan changing the weight of the various constraints, without modifying their position.

3.1.5 Comparison between ViTAT and tangential fields

The comparison between ViTAT plans and TF ones was carried out analyzing the dose parameters extracted from DVHs for both OARs and PTV. The parameters under analysis were mean dose (D_m), maximum dose ($D_{1\%}$ for CTV/PTV and $D_{2\%}$ for OARs) and selected DVH parameters. $V_{95\%}$ was used as PTV coverage indicator, while PTV homogeneity was evaluated using the standard deviation of its dose distribution. Concerning OARs, $D_{2\%}$, punctual maximum dose (D_{max}), mean dose (D_m) and $V_{5\text{Gy}}$ for ipsilateral lung; $D_{2\%}$, D_{max}, D_m and $V_{3\text{Gy}}$ for heart; $D_{2\%}$, D_{max}, D_m for contralateral lung; $D_{2\%}$, D_{max}, D_m and $V_{5\text{Gy}}$ for contralateral breast.

Another ESAPI script was used to export semi-automatically all these parameters and DVHs and they were stored in a spreadsheet for analysis.

The comparison between ViTAT and TF took place separately for the right and left breast and significance of the distribution is evaluated using a two-tailed paired t-test considering p-vaules lower than 0.05.

3.1.6 Deliverability of ViTAT plans

ViTAT plans stress the machine to work only in a small portion of the arc. In order to assess whether the ViTAT plans are deliverable, dosimetry QA tests were performed, according to our QA procedures [95].

10 VITAT plans of 10 randomly selected patients among the ones considered for the study were verified. The dose distribution was measured in a planar phantom using a two-dimensional detector array (MapCHECK 2, Sun Nuclear; Melbourne, Florida, USA) inserted in the MapPHAN

Initial optimization templates

	Right-sided breast		*Left-sided breast*	
Organs:	Parameter	Priority	Parameter	Priority
Target	$D_{100\%}$	250	$D_{100\%}$	250
	D_{max}	410	D_{max}	410
PTV	$D_{100\%}$	420	D_{max}	420
Ipsilateral	$V_{40\text{Gy}}$	180	$V_{40\text{Gy}}$	180
Lung	$V_{30\text{Gy}}$	180	$V_{30\text{Gy}}$	180
	$V_{20\text{Gy}}$	250	$V_{20\text{Gy}}$	250
	$V_{16\text{Gy}}$	450	$V_{16\text{Gy}}$	450
	$V_{10\text{Gy}}$	200	$V_{10\text{Gy}}$	200
	$V_{5\text{Gy}}$	300	$V_{5\text{Gy}}$	300
	$V_{3\text{Gy}}$	180	$V_{3\text{Gy}}$	180
	$V_{2\text{Gy}}$	180	$V_{2\text{Gy}}$	180
	D_m	200	D_m	200
Contralateral	$V_{3\text{Gy}}$	180	$V_{3\text{Gy}}$	180
Lung	$V_{2\text{Gy}}$	100	$V_{2\text{Gy}}$	100
	$V_{1\text{Gy}}$	100	$V_{1\text{Gy}}$	100
	D_m	180	D_m	180
Contralateral	$V_{3\text{Gy}}$	200	$V_{3\text{Gy}}$	200
Breast	$V_{2\text{Gy}}$	400	$V_{2\text{Gy}}$	400
	$V_{1.7\text{Gy}}$	250	$V_{1.7\text{Gy}}$	200
	D_m	250	D_m	250
Heart	$V_{3\text{Gy}}$	200	$V_{38\text{Gy}}$	200
	$V_{2\text{Gy}}$	400	$V_{30\text{Gy}}$	250
	$V_{1.7\text{Gy}}$	250	$V_{20\text{Gy}}$	250
	D_m	250	$V_{10\text{Gy}}$	380
			$V_{5\text{Gy}}$	400
			$V_{2.5\text{Gy}}$	250
			D_m	250
Body	D_{max}	600	D_{max}	600

TABLE 3.1. Template used as a starting point for right and left breast case optimization. For the OARs the value of each parameter is obtained from the corresponding TF plan. D_m and D_{max} stand for mean dose and maximum dose respectively. In our protocol D_{max} is set to 40 Gy.

phantom. MapCHECK2 consists in 1527 diodes (active volume of 0.019 mm^3) in a 32 × 26 cm^2 uniformly spaced by 7.07 mm. The comparison between the measured and the calculated dose distribution was accomplished using the gamma index metrics with 3% and 3 mm clinical criteria.

3.2 KB-ViTAT model: training and validation

After studying the ViTAT technique, KB-models were implemented with the purpose of allowing autoplanning for right and left-sided whole breast replacing the manual TF planning.

3.2.1 ViTAT geometric configuration

In section 3.1 the ViTAT technique has been extensively described. Based on the results obtained on the feasibility study, discussed later, the following parameters have been selected for the KB model generation and application.

In short, ViTAT plans consisted of 4 arcs delivering 6 MV photon beams using a collimator rotation angle of ± 10° . Start and stop angles were set to 60° and 220° for the right-sided breast case and 300° and 135° for the left-sided one. Inverse planning optimization was carried out using the RA module of Eclipse™ TPS system (v. 13.6, Varian Inc.) using the AcurosXB© algorithm for dose calculation. Irradiation through the whole arc is inhibited apart from the first and last 20° of rotation. As previously explained, a new target structure is obtained expanding the PTV in the anterior and lateral direction towards the surface by 1.5 cm and a virtual bolus with 1.5 cm thickness and −500 HU is used. The bolus is removed before dose calculation.

3.2.2 KB-model generation

Patients treated in the period 2016-2020 were selected. The corresponding TF clinical plans were used to generate the KB-model. For the right-sided breast case 90 plans were considered (70 with physical wedged fields and 20 with FIF) and 103 TF plans (82 with physical wedged fields and 14 FIF) for the left-sided one.

These plans allowed us to generate two KB-models, one for the right-sided and one for the left-sided breast using the RapidPlan (RP) tool implemented in our TPS. The available pool of patients was large enough to guarantee also sufficiently numerous sets of plans for validation, considering both FIF (2019-2020) and TF(before 2016) plans, as later further discussed.

In order to generate a KB model, the system needs plans obtained with inverse planning modality and delivered with IMRT/VMAT technique. It was then necessary to link the original dose distribution of the clinical TF plans to a “fake arc” geometry that recalled the ViTAT geometry [32], consisting in two partially reverse arcs in the range 60°/220° and 300°/135° for right-side and left-side case respectively, with collimator rotation angle of ± 10° . Start and stop angles were chosen according to the population distribution of beam angles of the clinical TF plans, as explained before.

As mentioned in chapter 1, RP considers overlay in a certain direction depending on the arc geometry, for this reason the avoidance sectors were not set in this phase, so to consider all the BEV projections in all the directions of the arc, not only the first and last 20° .

Since for simplicity only two arcs were considered, the impact on DVH estimates (DVHE) of using a different number of arcs for building and validating the model was investigated. Since the BEV projections and OAR partitions are the same for equal arcs geometry, no differences were observed in the DVHE for model configuration using two arcs instead of four arcs as expected for the ViTAT technique. The OARs considered in the model were the ipsilateral lung, contralateral breast for the right side and with the addition of the heart for the left side. Other OARs such as right-side heart and contralateral lung, were not considered in the model, but they were added in the final planning template with fixed constraints for all patients (see later). Due to the arc orientations and the treatment ballistic, they are not inside the BEV of the arc, making it difficult to consider them in the model.

The tuning of the model and outlier removal were performed using the two Varian software: RP system and Model Analytic platform. As reported in literature [31, 71, 96] for each OAR a regression plot is created showing the relation between the scores of the first component of the PCA analysis for the geometry of the organ and the corresponding DVH for each patient. If these values exceed by more than 2 standard deviations from the fitted principal component curve, the corresponding patient would be considered as an “outlier”. As mentioned in subsection 1.2.3 only geometric outliers are kept inside the model because they are considered important to have a representative of an “uncommon” but clinically suitable anatomical condition.

3.2.3 Template for automatic ViTAT plan optimization

For each OAR, RP generates the DVHEs that are given as a band showing the confidence interval of the expected DVH. The generated constraints that are suggested by the system are taken in correspondence of the lower band. A fine tuning process is fundamental to obtain a robust and efficient template. For each side, a tentative template creating automatic plans for five sample patients was generated, trying to find the optimal position and penalty of the generated DVH constraints. At every modification, the template is tested on the five patients until a final solution is found to work optimally for all of them. This process proved to be successful in other studies. [31][67][97] As a main criteria for template modification, once fixed the PTV priorities, the OARs priority were gradually increased, creating different test templates. Comparison between templates was done in terms of the final plan obtained after the optimization process without further modification of the test template. Relevant dose-volume parameters were selected and analyzed for the sample of five test patients, against the original clinical plans in order to assess the performances of the best test template.

3.2.4 Validation tests

In order to clinically apply the model it is necessary to validate it. An external validation has been performed on 60 new patients equally divided between right-sided and left-sided breast. Patients were selected between those who were treated in the range 2019-2020 and 2013-2016, so to validate the model for both the FIF plans and wedged fields ones, respectively.

The number of FiF plans in the validation samples is 15 for the right-sided breast case and 11 for the left-sided one. On the other hand, the number of wedged plans is 15 and 19 for the right and left case respectively.

It is possible to automate the ViTAT optimization process using the DVHE obtained from the KB models. To do so it is extremely crucial to assess the performances of the models in adapting to the anatomical and morphological features of each individual patient. As normally done in literature [23][66][31][32], the validation is carried out by optimizing a certain number of clinical TF plans using the ViTAT technique with the template associated with the model and comparing the results with the original plan. The comparison between the clinical TF plan and the KB fully-automatic ViTAT plans (KB-ViTAT) was carried out in terms of dose-volume parameters analogously to what was done for the feasibility study in section 3.1.5: mean dose (D_m), maximum dose ($D_{1\%}$ for PTV and $D_{2\%}$ for OARs) and other parameters to take into account for the shape of the whole DVH for ipsilateral OARs. As previously introduced, all parameters and DVHs were semi-automatically exported via ESAPI scripts and stored in spreadsheets for analysis. To assess the statistical significance (associated with p-value lower than 0.05) of the differences between the two populations, two-tailed paired t-tests were performed.

3.3 KB-model in Tomo Direct

Once implemented, the ViTAT KB-model was also applied to the TomoTherapy® system from Accuray®, Inc. to test its prediction performances on another system. Moreover a new KB-model was generated on the Eclipse™ TPS system (v. 13.6, Varian Inc.) specifically for the TomoTherapy® system for whole breast irradiation.

The machine system used is the TomoHD™ (v.2.1.4) delivering 6 MV Flattening-Filter-Free beams, coupled with the v5.1.1.6 Planning Station. All patients were treated using the TomoDirect™ (TD) modality that allows the generation of IMRT-like plans with high conformity and homogeneous target coverage. [98–100]. Daily IGRT is achieved with a MegaVoltageCT for all patients;

Many parameters could affect plan quality and delivery time, such as the field width, pitch value, modulation factor and number of fields used. These values are set by the planner and may vary a lot from plan to plan. In our institute the field-widths normally used for breast cancer treatment are 5 cm and 2 cm. The pitch value modifies the couch speed, the modulation factor works on the maximum aperture time of leaves of the MLC. Incrementing the number of fields,

changing slightly its angle position by 5° -10° , it is possible to increment coverage and PTV dose homogeneity. At least 2 beams are used, generally up to a maximum of 4.

In TD modality the leaves of the MLC towards air are opened to maximum value settable on the machine to account for intra and inter-fraction deformability.

3.3.1 ViTAT model in Tomo environment

A set of 35 patients treated for right-sided breast cancer and 66 for the left-sided one, was selected in the period 2017-2021 for ViTAT model prediction evaluation. For each patient a ViTAT plan setup was prepared inside the Eclipse™ TPS, as described in subsection 3.1.1 and 3.2.1. The previously created KB-model (ViTAT-KB-model) was applied using he RP tool and the prediction was generated for ipsilateral lung and left-sided case heart.

For each OARs the tool generates two bands, lower and upper, showing the region where the DVH will most likely land for the considered anatomy (see subsection 1.2.1). The average value between these higher and lower bands (predicted mean DVH) has been used for statistical analysis.

At the same time, the dose distributions of the clinical plans of these patients have been exported from the Tomo TPS and reimported in the ViTAT Eclipse plan maintaining the original normalization, in order to highlight the differences between prediction and clinically achieved DVHs.

The comparison between the DVH of clinical TD plans (TD-DVH) and the one obtained from the prediction (KB-TD-DVH), was conducted for every patient in terms of mean dose (D_m) and evaluating the differences between clinical and predicted values along the DVH curves for the whole population. At every dose point the distribution has been studied analyzing the 25/75 quantile and the maximum and minimum values of the population were considered, excluding some outlier patients detected using the generalized extreme studentized deviate test for outliers.

Prediction data and clinical DVHs have been exported using a semiautomatic ESAPI [101] script into a spreadsheet and further analysis have been performed using MATLAB®.

3.3.2 Dedicated KB-model generation for left-sided case

A dedicated KB-model has been generated for left-sided breast cancer treatment following the criteria introduced in subsection 3.2.2. In short, a fake ViTAT plan geometry has been set in the Eclipse™ TPS, with arcs spanning in the range between 300° and 135°. The dose distribution of the clinical TD plans was exported from the Tomo system and was reimported in Eclipse™, being linked to the fake ViTAT plan.

A total number of 79 patients treated for left-breast cancer in TD modality were found . A set of 69 patients containing the previously introduced set of 66 patients has been used as training set, leaving out 10 patients as an external validation set Considering the small numbers of the

right-sided breast cancer set, it was decided to postpone the generation of the model for the right-sided breast case.

As discussed in chapter 1, the RP system creates a regression model for each selected structure. The OARs selected were ipsilateral lung, heart, contralateral breast and contralateral lung. The regression model will show the relation between the scores of PCs for both the DVH and the GEDVH for the training set of patients.

As introduced in subsection 3.2.2, the model was tuned using the tools inside the RP environment and the Model Analytic Platform from Varian. Outliers were detected and eliminated only if they were considered "dosimetric" outliers, being associated with a suboptimal plan. On the other hand the "geometric" outliers were kept inside the training set as a representative case for a possible but uncommon anatomy.

3.3.3 Creation and fine tuning of template

As described in chapter 1, RP shows the prediction with a lower and an upper band, highlighting the region where the DVH would most likely land. The regression model prediction was used to generate a template. Objectives were generated using the values slightly below the lower band, in correspondence of opportunely selected dose or volume values. It is fundamental to choose the position of the objective wisely.

The templates in Eclipse™ TPS are different from the ones in Tomo TPS. In Tomo the optimizer manages the overlapping voxels of ROIs considering the geometrical priority assigned to that contour: voxels are assigned to the structure with the higher priority.

Concerning the cost function, the Tomo TPS associates every ROI to different kinds of coefficients: a parameter called importance, that increments the weight of the whole structure; the maximum dose value and its penalty; certain dose-volume parameters and their penalties.

Following the same approach discussed in subsection 3.2.3, five sample patients were selected from the training set and automatic plans were created for the five patients. Iteratively the template was modified in terms of modulation factor, pitch, objective position, importance coefficients and penalties in order to reach the optimal configuration for the whole testing sample and for each testing patient.

The template was generated in the Eclipse™ environment when launching the model calculation in the RP module. Successively it is automatically converted and sent to the TomoTherapy® planning station via ESAPI scripting. The complete automatic planning workflow is shown in Figure 3.2.

3.3.4 Model validation

An internal validation was performed randomly selecting 30 patients inside the training set, excluding the dosimetric outliers. A summarize of machine settable parameters used for the optimization of this plans are shown in table 3.2.

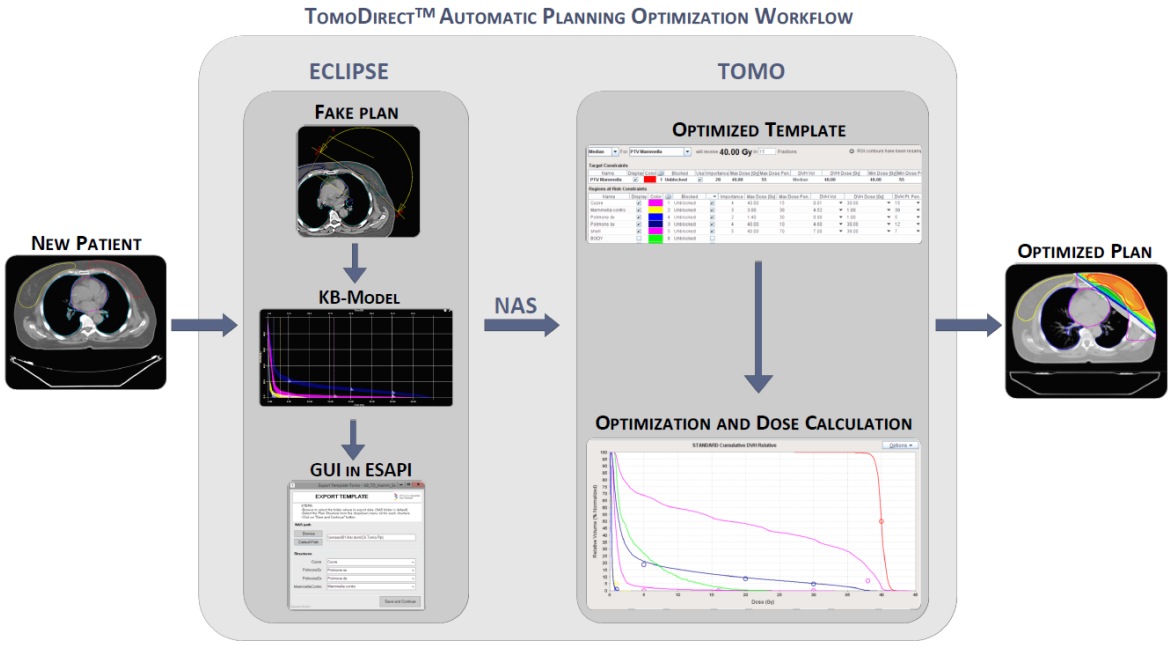

FIGURE 3.2. Scheme of automatic planning workflow for TomoDirect™ . A new patient data is uploaded in Eclipse TPS. A fake rotational geometry is used to obtain the prediction data using the KB-model in the RapidPlan Tool. A homemade script with graphic user interface allows to translate the prediction into a Tomo readable template. It is automatically sent to the Tomo station via Network Attached Storage (NAS). In tomo the template is used for the optimization process, in order to obtain the final automatically optimized plan.

TomoTherapy® planning parameters

Set	*Field Width*	*# plans*	*Pitch*	*Modul. Factor*	*Delivery time*
Internal Valid.	5 cm	20	[0.250 - 0.500]	[2.000 - 3.000]	6 ± 1 min
	2.5 cm	10	[0.251 - 0.350]	[1.800 - 3.500]	8 ± 2 min
External Valid.	5 cm	6	[0.250 - 0.500]	[2.000 - 3.500]	6 ± 1 min
	2.5 cm	4	[0.251 - 0.287]	[1.800 - 2.900]	9 ± 1 min

TABLE 3.2. Planning characterization of internal and external validation set, showing the number of plans, pitch value range, modulation factor range and delivery time (mean value and standard deviation) differentiating per field width used (5cm and 2.5cm).

The number of available patients in the range 2017-2021 was limited and only 10 patients were selected between those outside the training set to carry out an external validation.

For both internal and external case, model performances were evaluated comparing the generated (KB-TD) plans with respect to the clinical (TD) ones in terms of dose-volume parameters analogously to what was previously described: $D_{1\%}$,$V_{95\%}$ and STD for PTV; D_m and $D_{2\%}$ for OARs plus some specific dose-volume parameters for the ipsilateral lung and heart. As aforementioned, all parameters and DVHs were semi-automatically exported via ESAPI scripts and stored in spreadsheets for analysis. To assess the statistical significance (associated with p-value lower than 0.05) of the differences between the two populations, two-tailed paired t-tests were performed.

CHAPTER 4

RESULTS

In this chapter the reader's attention will be focused on the results obtained in the studies previously introduced. The same order presented in chapter 3 will be followed.

4.1 ViTAT feasibility study

4.1.1 Optimized geometry parameters

Analyzing the values for the angle position distribution over the clinical TF plans, the modal medial and distal angles were found to be 55° and 230° respectively for right breast irradiation, and 300° and 125° respectively for the left-sided breast case.

This suggests that the optimal angles ranges to be used are [65°, 45°] and [220°, 240°] for right breast and [290°, 310°] and [115°, 135°] for the left side, in order to usefully exploit the 40° (20° + 20°) of irradiation of the arc. In addition, based on our experience, the medial starting angle was shifted to [60° , 40°] and [295°, 315°] for right and left sided breast, respectively, in order to limit any risk of collision with the gantry or to avoid treatment to be stopped by the interlock for vicinity to the patient.

The distribution and the selected range for the angle position is shown in Figure 4.1.

4.1.2 Virtual bolus selection

Regarding the pre-study evaluation on virtual bolus definition, among the six combinations the bolus characterized by a thickness of 1.5 cm and a density of −500 HU, was selected for our purposes.

Differences in the results were pretty similar, but the chosen one was associated with the lowest mean dose (up to 5% better) and lowest $D_{2\%}$ (up to 7% better) for OARs, and best coverage

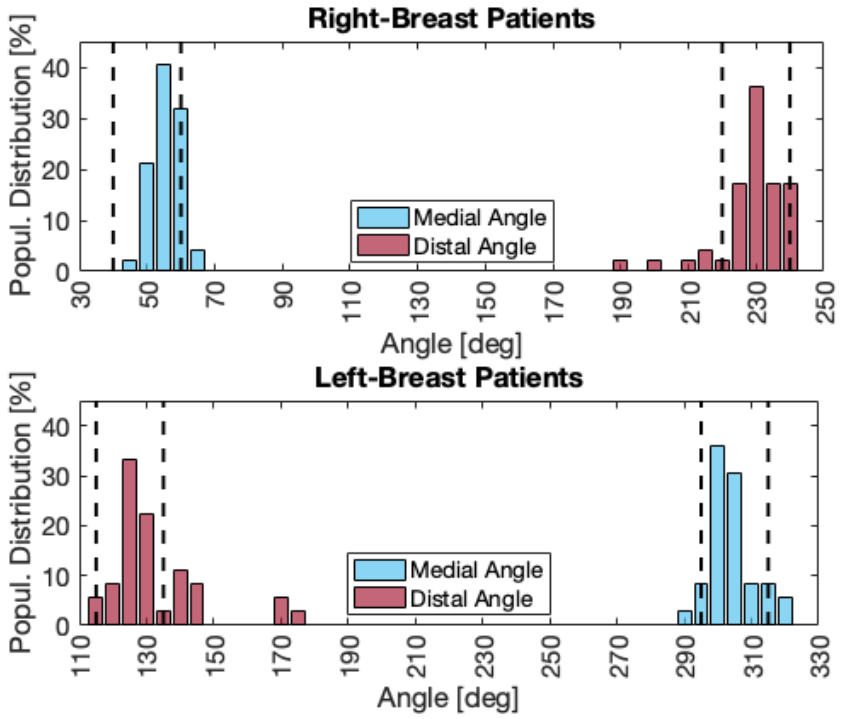

FIGURE 4.1. Population distribution of medial and distal beam angles chosen for TF plans. Right-sided breast case on top and left-sided one on the bottom. The dashed black lines are highlighting the chosen range for ViTAT plan irradiation.

to PTV (up to 3% better) with respect to other bolus characteristics. The expansion of 1.5 cm was high enough to assure target hit in case of intra and inter-fraction movements or deformation [102, 103].

4.1.3 ViTAT vs TF comparison

Differences between TF and ViTAT plans were small and in general slightly in favor of ViTAT (see Figure 4.2 and Tables 4.1 and 4.2). In order to better appreciate the dose distribution differences some few representative cases are shown in Figure 4.3.

Right-sided breast case

Similar PTV coverage was achieved for TF and ViTAT. PTV $D_{1\%}$ was improved by 1% with ViTAT (p-value < 0.05). PTV dose homogeneity was improved (1SD: 0.1 Gy, p-value < 0.05). Ipsilateral lung mean dose was similar (6.8 Gy vs 6.9 Gy, p = 0.2): there was a modest worsening (about 3% volume averaging) for the ipsilateral lung in the 2-15 Gy range, and a slight improvement (about 1% volume averaging) in the 20-35 Gy range. Contralateral OARs were better spared by ViTAT plans: ViTAT mean doses of heart, left lung and left breast were lowered by 19%, 11% and 35% respectively, namely 0.2 Gy, 0.1 Gy, 0.3 Gy.

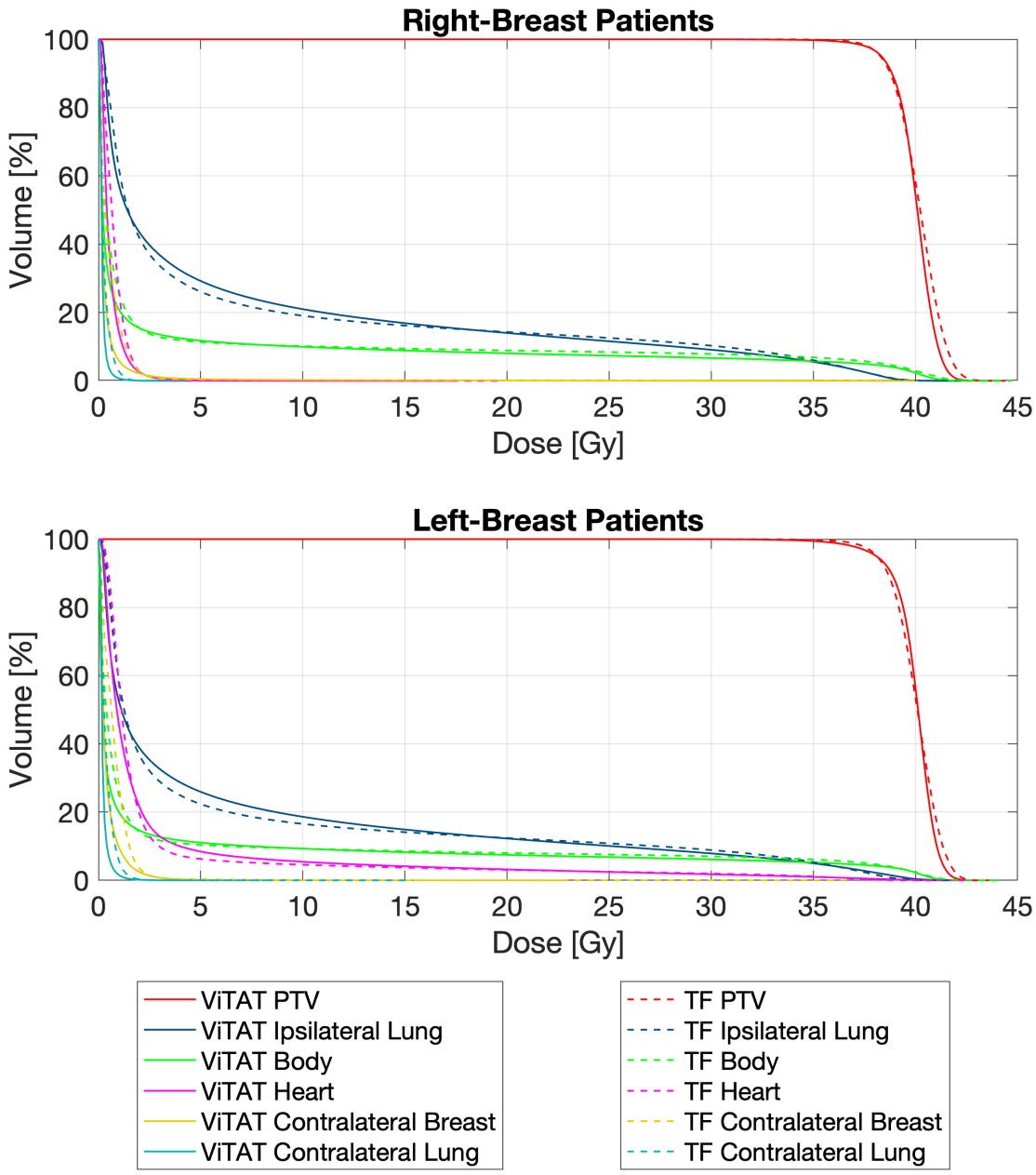

FIGURE 4.2. DVH curves averaged over the whole population for right (top) and left (bottom) breast patients. Solid lines refer to ViTAT plans and the dashed ones refer to TF plans.

Dose-Volume parameters - ViTAT vs TF - Right-Breast case				
Organ	*Parameter*	*TF*	*ViTAT*	ΔP
PTV	$V_{105\%}$[%]	3.6 ± 3.0	0.7 ± 1.0	**2.9**
	$V_{98\%}$[%]	86.3 ± 4.6	87.8 ± 3.9	−1.5
	$V_{95\%}$[%]	96.7 ± 1.7	96.7 ± 1.6	0.0
	$D_{99\%}$[Gy]	37.2 ± 0.7	36.9 ± 1.0	0.3
	$D_{1\%}$[Gy]	42.3 ± 0.4	41.8 ± 0.3	**0.5**
	SD [Gy]	1.1 ± 0.1	1.0 ± 0.2	**0.1**
Contralateral	$D_{2\%}$[Gy]	1.0 ± 0.4	0.7 ± 0.3	**0.3**
Lung	D_m[Gy]	0.3 ± 0.1	0.2 ± 0.1	**0.2**
Ipsilateral	$V_{20\text{Gy}}$[%]	14.3 ±3.0	14.0 ± 2.7	0.3
Lung	$V_{5\text{Gy}}$[%]	26.1 ± 4.1	29.2 ± 3.8	**−3.1**
	$D_{2\%}$[Gy]	37.5 ± 1.2	37.5 ± 1.2	0.0
	D_m[Gy]	6.8 ±1.2	6.9 ± 1.0	-0.1
Contralateral	$D_{2\%}$[Gy]	3.4 ± 7.3	2.5 ± 4.1	0.9
Breast	D_m[Gy]	0.6 ± 0.4	0.4 ± 0.4	**0.2**
Heart	$D_{2\%}$[Gy]	1.9 ± 0.6	1.9 ± 0.8	0.0
	D_m[Gy]	0.8 ± 0.3	0.6 ± 0.2	**0.2**
Body	D_{1cc}[Gy]	42.9 ± 0.5	42.5 ± 0.4	**0.4**
	D_m[Gy]	4.0 ± 1.2	3.7 ± 0.8	**0.3**

TABLE 4.1. Comparison between ViTAT and TF in terms of average dose-volume parameters for right-sided breast case.

Dose-Volume parameters - ViTAT vs TF - Left-breast case				
Organ	*Parameter*	*TF*	*ViTAT*	ΔP
PTV	$V_{105\%}$[%]	2.0 ± 2.2	0.5 ± 0.5	**1.5**
	$V_{98\%}$[%]	84.2 ± 3.0	87.8 ± 2.7	**−3.6**
	$V_{95\%}$[%]	95.7 ± 1.6	95.4 ± 2.0	0.3
	$D_{99\%}$[Gy]	36.7 ± 1.0	36.1 ± 1.1	**0.6**
	$D_{1\%}$[Gy]	42.0 ± 0.3	41.8 ± 0.2	**0.2**
	SD [Gy]	1.1 ± 0.1	1.0 ± 0.1	**0.1**
Contralateral	$D_{2\%}$[Gy]	1.2 ± 0.4	0.9 ± 0.3	**0.3**
Lung	D_m[Gy]	0.4 ± 0.2	0.2 ± 0.1	**0.2**
Ipsilateral	$V_{20\text{Gy}}$[%]	12.4 ± 3.7	12.3 ± 4.1	0.1
Lung	$V_{5\text{Gy}}$[%]	22.4 ± 4.9	26.0 ± 5.5	**−3.6**
	$D_{2\%}$[Gy]	37.0 ± 2.0	37.1 ± 2.9	0.1
	D_m[Gy]	6.0 ± 1.4	6.2 ± 1.6	0.2
Contralateral	$D_{2\%}$[Gy]	2.3 ± 1.3	2.1 ± 0.8	0.2
Breast	D_m[Gy]	0.8 ± 0.3	0.4 ± 0.1	**0.4**
Heart	$V_{3\text{Gy}}$[%]	9.8 ± 6.5	12.9 ± 6.5	**−3.1**
	$V_{16\text{Gy}}$[%]	3.6 ± 2.5	3.9 ± 3.0	−0.3
	$D_{2\%}$[Gy]	23.4 ± 13.1	23.0 ± 12.1	0.4
	D_m[Gy]	2.5 ± 1.0	2.5 ± 1.3	0.0
Body	D_{1cc}[Gy]	42.6 ± 0.4	42.4 ± 0.3	**0.2**
	D_m[Gy]	3.7 ± 0.9	3.4 ± 0.9	**0.3**

TABLE 4.2. Comparison between ViTAT and TF in terms of dose-volume parameters. Average value among the patient populations for left-sided breast case. Mean value ± standard deviation values are shown. Bold font is used for significant ($p<0.05$) differences between TF and VITAT population.

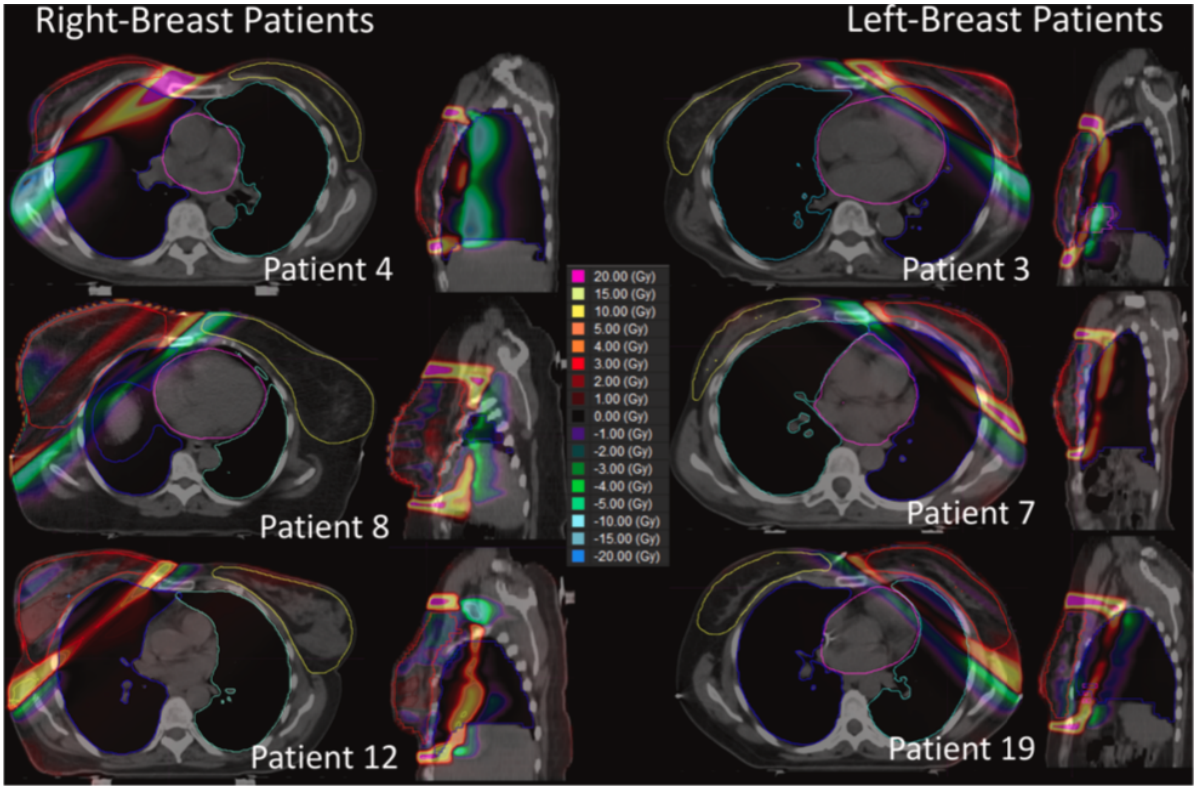

FIGURE 4.3. Dose distribution differences for few relevant left and right-sided breast cases between ViTAT and TF plans. The bluish palette is associated with negative values, meaning that ViTAT delivers a higher dose than TF, while the yellow-reddish palette is associated with positive values to a lesser delivered dose.

Left-sided breast case

Left-sided breast plans achieved similar results as for the right-cases. PTV coverage was similar, PTV $D_{1\%}$ and dose homogeneity were improved (1% with ViTAT and 1SD: 0.1 Gy, p-value $<$ 0.05, respectively). Ipsilateral lung mean dose was similar (6.0 Gy vs 6.2 Gy) showing the same worsening and improvement range as the right- case. Heart mean dose was 2.5 Gy for both ViTAT and TF plans. Right breast and right lung lowered their mean dose by 34%, namely 0.3 Gy and 0.2 Gy respectively.

For both right and left-sided breast cases, body integral dose was 7% lower for ViTAT plans with respect to TF ones. This is mostly due to the improved conformity of ViTAT dose distributions compared to TF, as also shown in Figure 4.3.

Selected OARs dose/dose-volume values delivered with ViTAT were compared to the corresponding values delivered with TF. Differences in mean DVHs were shown in Figure 4.4: the percentage difference was shown along the DVH curve with a 0.1 Gy step, point by point. The

ViTAT deliverability	
# patient	*γ index [%]*
1	98.7
2	98.5
3	99.6
4	99.6
5	99.9
6	99.9
7	99.7
8	99.9
9	99.5
10	99.8
Mean	99.5 ± 0.5

TABLE 4.3. ViTAT deliverability verification. γ index measured for 10 plans considering 3% of dose and 3 mm as parameters. The last row is showing the average value and the standard deviation of the considered sample.

grey areas highlight significant differences ($p < 0.05$), found by calculating the p-value for each dose point over the patient population. Figure 4.5 shows differences in OAR mean doses and PTV homogeneity for each patient. Patients are ordered chronologically, showing that apparently more recent clinical plans are nearer to ViTAT performances while the oldest ones were slightly worse. This most likely depends on the prevalence of field in field techniques in the most recent ones.

4.1.4 ViTAT deliverability

ViTAT deliverability was verified through patient-specific quality assurance (QA) procedure according to Rinaldin et al. [95]. Verification at our accelerator CLINAC-IX 2300 in Rapid Arc (VMAT) modality, was carried out on 10 randomly selected plans, following the QA institutional procedure. The dose distribution calculated by the TPS was compared against the delivered one as measured in a planar phantom using a two-dimensional detector array (MapCHECK 2, Sun Nuclear Corporation).

All plans correctly delivered the expected dose distribution without triggering any interlock, interruptions or errors. The gamma rate (thresholds of 3% - 3 mm) was registered and the average value was 99.5% ± 0.5%, and in general always higher or equal to 98.5% (see Table 4.3), comparing well against our experience in patient QA of VMAT with an average value of 97% ± 3% [95].

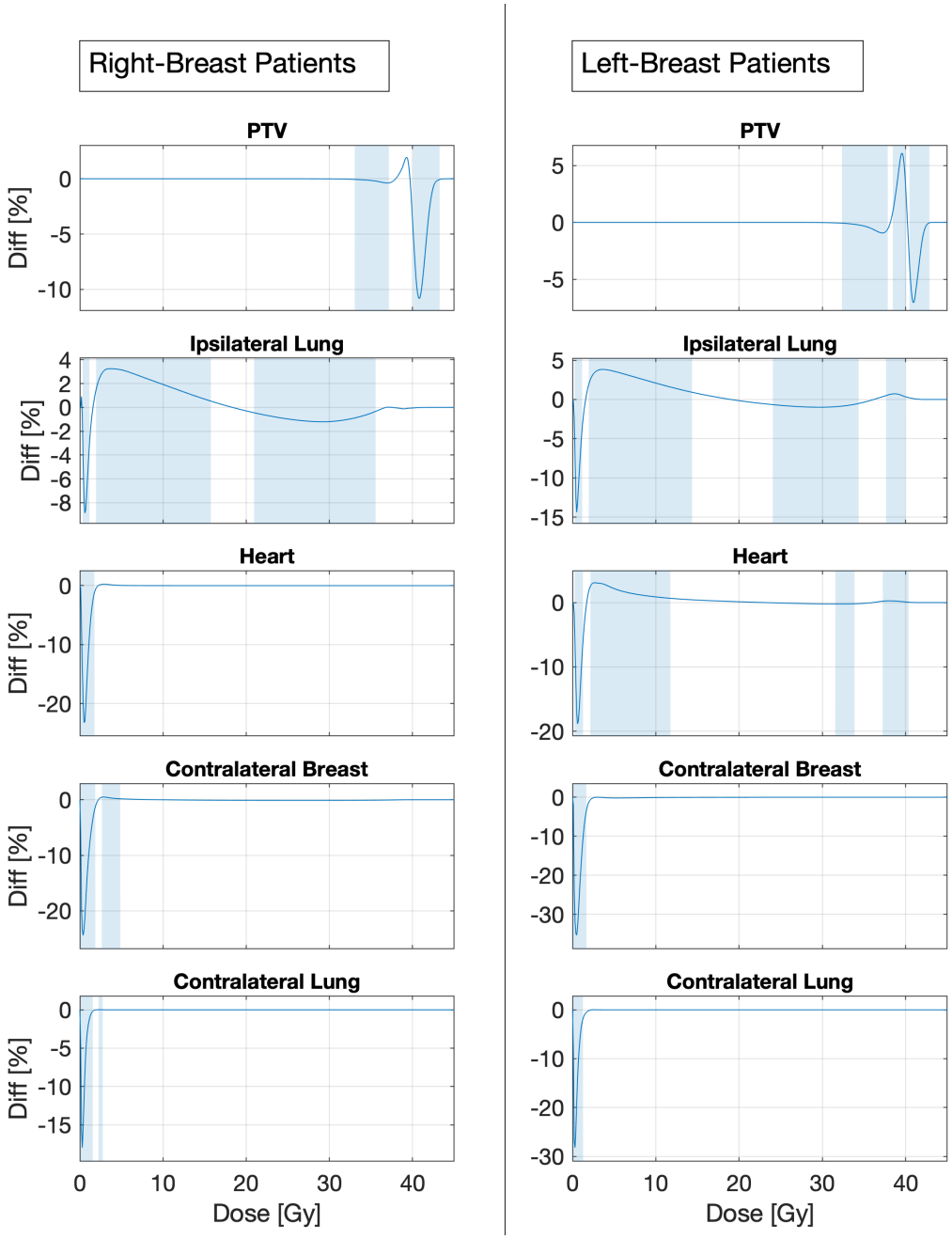

FIGURE 4.4. Percentage differences in ViTAT and TF DVHs (negative deviations mean that ViTAT is better than TF). The light blue regions highlight the significant differences ($p < 0.05$).

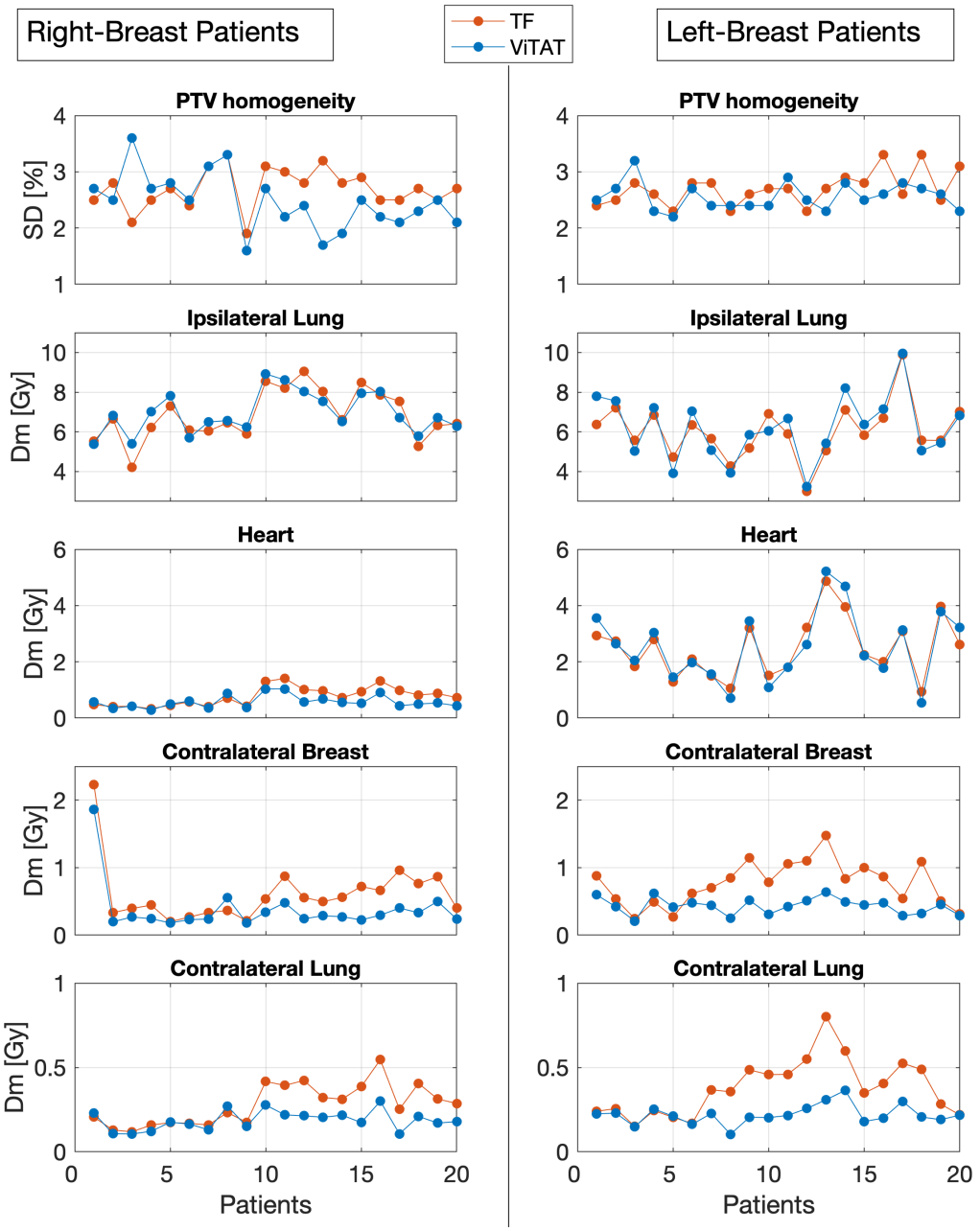

FIGURE 4.5. Patient-by-patient comparison between ViTAT (blue line) and TF (orange line) PTV homogeneity and OARs mean doses.

4.2 KB-ViTAT model: training and validation

4.2.1 KB-models and templates generation

Two models were generated, one for the right breast and one for the left breast cancer treatment. Performing outlier exclusion, 10 patients (out of 90, right-sided breast case) and 18 patients (out of 103, left-sided breast case) were excluded by the model being associated with sub-optimal plans for at least one of the considered OARs.

The regression plots for ipsilateral OARs for the final model are shown in Figure 4.6. The obtained χ^2 and R^2 are shown in Table 4.4: contralateral OARs have a lower R^2 with respect to the ipsilateral OAR because they are not always visible from the BEVs of the fields.

The templates were fine-tuned using DVHEs obtained from models and resulting DVHs after automatic optimization. Concerning ipsilateral OARs and Contralateral Breast objectives were generated using the RapidPlan™ tool, while for not trained OARs, position and penalties of DVH constraints were fixed and tuned as previously explained (subsection 3.2.3), as shown in Tables 4.5 and 4.6.

4.2.2 External Validation

The comparison between KB-ViTAT and TF plans is shown in Figure 4.7, where the mean DVHs over 30 new patients for both right and left case respectively were calculated. Among the 30 KB automatic plans per side, one for the right case and seven for the left case were considered unacceptable in terms of PTV coverage and/or ipsilateral lung constraints. This was due to the position of PTV with respect to the OARs causing an insufficient coverage of the medial part of the PTV. It is important to notice that after a manual refinement of the start and stop angles of 5° or 10° by an expert planner, all automatic KB-ViTAT plans resulted in acceptable and well fitted TF-performances. A refinement of the medial angle of 5° was sufficient in the right case and in four left cases, obtaining the following angles, respectively: 65°/220° and 295°/135°. The remaining three left-sided breast patients required also a modification of the distal angle by

Model regression parameters

Model	*Structures*	χ^2	R^2
Right-sided breast	Ipsilateral Lung	1.043	0.604
	Contralateral Breast	1.050	0.511
Left-sided breast	Ipsilateral Lung	1.043	0.723
	Heart	1.035	0.672
	Contralateral Breast	1.046	0.505

TABLE 4.4. Regression parameters for each OARs inside the right and left-sided breast models.

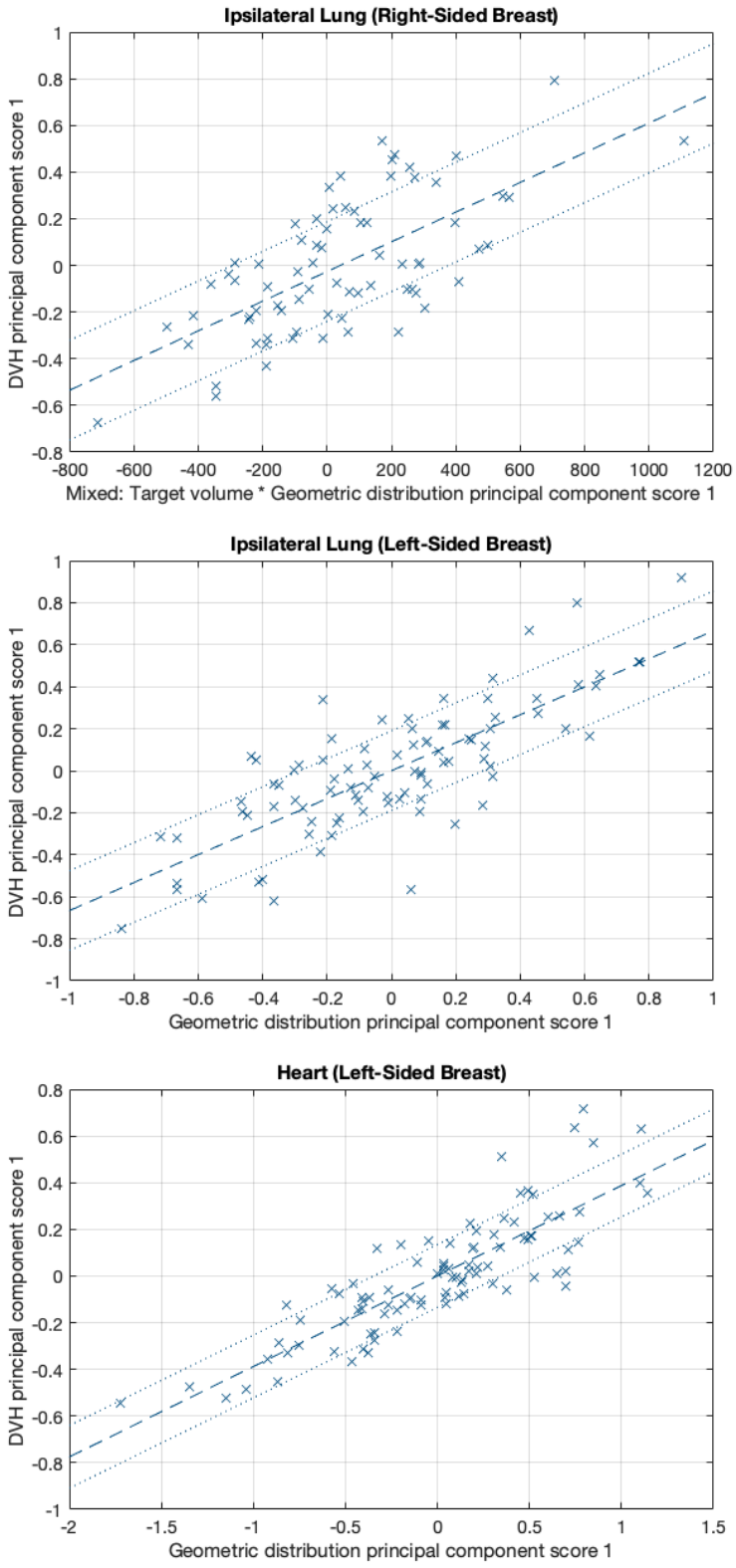

FIGURE 4.6. Regression plots for ipsilateral OARs inside the right-side and left-side models. Starting from the top: ipsilateral lung for the right case, ipsilateral lung and heart for the left case.

Right-sided breast cancer treatment template

Organ	*Objectives*	*Volume [%]*	*Dose [Gy]*	*Priority*	*gEUD a*
PTV	Upper	0	40	500	
	Lower	100	40	500	
Target	Upper	0	40	500	
	Lower	100	40	500	
Contralateral	Upper	0	3	600	
Lung	Upper	2.5	1	150	
	Upper	10	0.7	150	
	gEUD		0.3	200	1
Contralateral	Upper	Generated	1.5	600	
Breast	Upper	Generated	1	200	
	Upper	0	Generated	400	
	gEUD		0.5	500	1
Heart	Upper	0	3	600	
	Upper	2.5	1	150	
	Upper	10	0.7	150	
	gEUD		0.5	200	1
Ipsilateral	Upper	0	40	200	
Lung	Upper	Generated	30	200	
	Upper	Generated	20	200	
	Upper	Generated	16	500	
	Upper	Generated	10	400	
	Upper	Generated	5	500	
	Upper	Generated	2	500	

TABLE 4.5. KB-ViTAT fine-tuned optimization template for right-sided breast.

Left-sided breast cancer treatment template

Organ	*Objectives*	*Volume [%]*	*Dose [Gy]*	*Priority*	*gEUD a*
PTV	Upper	0	40	600	
	Lower	100	40	600	
Target	Upper	0	40	600	
	Lower	100	40	600	
Contralateral	Upper	0	3	600	
Lung	Upper	2.5	1	150	
	Upper	10	0.7	150	
	gEUD		0.3	200	1
Contralateral	Upper	Generated	1	500	
Breast	Upper	Generated	1.5	250	
	Upper	0	Generated	450	
	gEUD		0.5	550	1
Heart	Upper	0	40	250	
	Upper	Generated	30	250	
	Upper	Generated	20	250	
	Upper	Generated	16	450	
	Upper	Generated	10	450	
	Upper	Generated	5	500	
	Upper	Generated	2	500	
	gEUD		3.4	500	1
Ipsilateral	Upper	0	40	180	
Lung	Upper	Generated	30	180	
	Upper	Generated	20	180	
	Upper	Generated	16	450	
	Upper	Generated	10	400	
	Upper	Generated	5	450	
	Upper	Generated	2	450	

TABLE 4.6. KB-ViTAT fine-tuned optimization template for left-sided breast treatment. RapidPlan™ tool automatically replaces the parameters marked with the "Generated" placeholder. Fixed objectives were used for PTV, Target and contralateral lung.

5° (two cases) and 10° (one case).

Once the start/stop angles were modified, restarting the automated optimization, the plan resulted to be acceptable and comparable to the original clinical TF plan. In Figures 4.8 and 4.9 there are examples of the effect of these changes for the right and left case, respectively.

Quantitatively speaking, the results are shown in Tables 4.7 and 4.8. In general, differences between TF and KB-ViTAT plans were small and in slight favor of KB-ViTAT. PTV coverage was similar and PTV $D_{1\%}$ was improved with KB-ViTAT ($p < 0.05$). Contralateral OARs were better spared with KB-ViTAT, decreasing contralateral lung, breast and right-side heart mean dose by 33%, 20% and 14%, respectively, corresponding to a reduction of 0.1 Gy ($p < 0.05$). The KB-ViTAT integral dose to the body was improved: 5% lower for the right case and 8% for the left case. Concerning ipsilateral lungs, the DVHs show a few % modest worsening in the 2-15 Gy range and a slight improvement in the 20-35 Gy range for both right and left cases. Despite that, the mean dose did not change (Right: 6.8 Gy, $p > 0.05$; Left: 5.7 Gy, $p > 0.05$). A similar behavior was found for the left-side heart with a modest worsening in the range 2-10 Gy and a slight improvement in the range 15-35 Gy, while on average, delivering the same mean dose (2.7 Gy). Furthermore Figures 4.10 and 4.11 are representing population histograms highlighting the differences between TF and KB-ViTAT for the selected PTV/OARs dose-volume parameters. Moreover, the time for KB-ViTAT automatic plan optimization and final dose calculation was registered and found to be 12 ± 2 minutes. The time for the corresponding clinical TF plans were not available; however, based on our clinical experience, typical values of the time dedicated to manual plan optimization with wedges or field-in-field range between 1 and 3 hours.

Model performances were also evaluated separately for wedged fields plans (the oldest group) and the more recent FIF plans (delivered in 2019-2020). No statistically significant differences were found in terms of the PTV/OARs dose-volume parameters when comparing the differences between KB-ViTAT and TF in the two cohorts of plans.

4.2.3 Clinical implementation

The KB automatic approach for ViTAT was clinically implemented at our institute for both right and left (more recently) breast cancer treatment. Eight out of forty plans treated needed a manual refinement: four needed only a manual shift of the start and stop angles and for other four patients a further manual optimization refinement was carried out.

The first 40 clinical KB-VITAT plans underwent the same dosimetric verification before treatment. The gamma passing rate in comparing the calculated vs delivered dose maps was larger than 98% for all plans, considering 3% - 3 mm as criteria, in agreement with our experience [95].

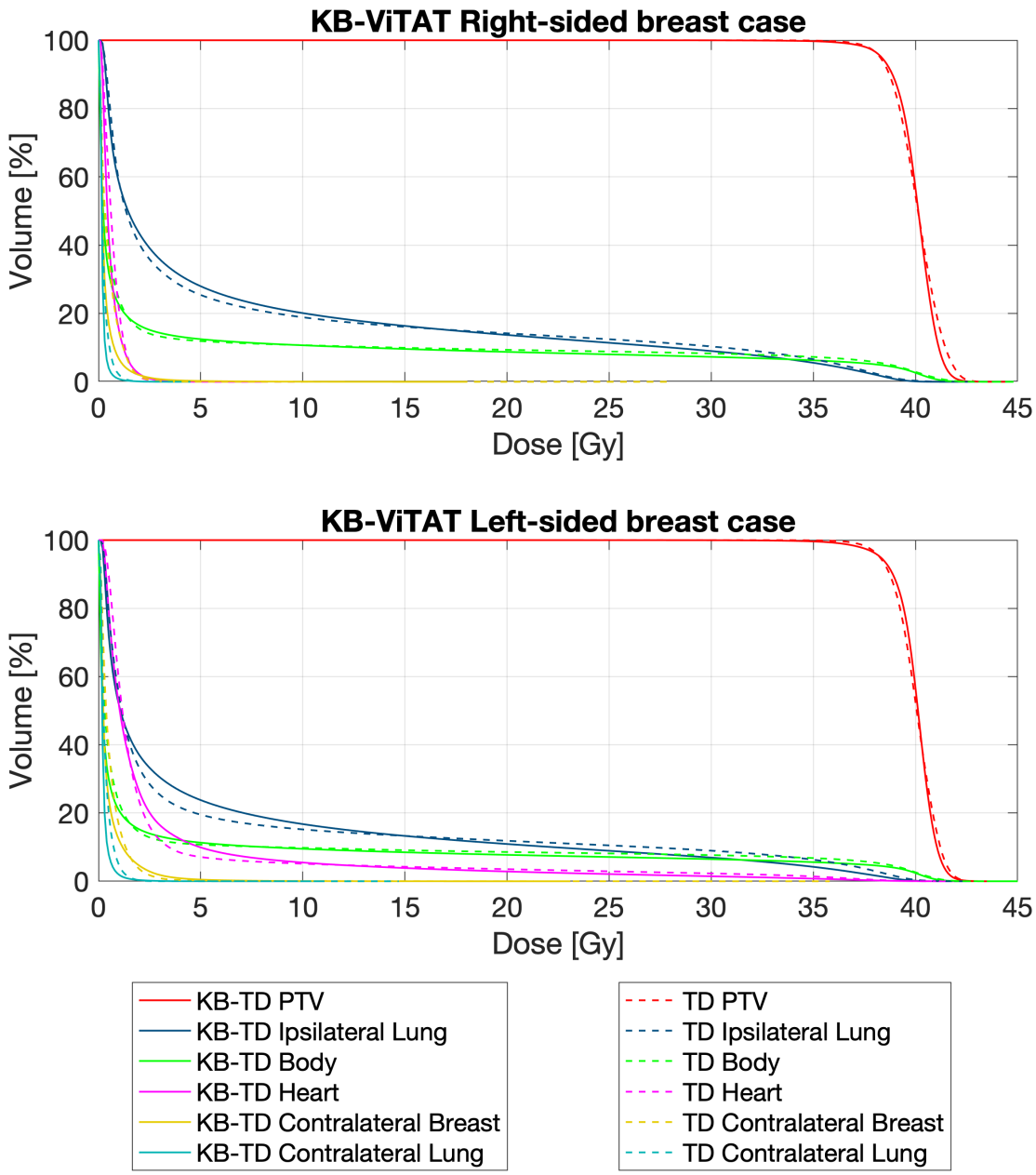

FIGURE 4.7. Mean DVHs over the 30 patients external validation set for KB-ViTAT (solid lines) and clinical TF (dashed lines) for right-sided (top) and left-sided (bottom) breast cases.

KB-ViTAT vs clinical TF (Right-side)

Organ	*Parameter*	*TF*	*KB-ViTAT*	ΔP
PTV	$V_{95\%}$ [%]	96.7 ± 1.3	96.7 ± 0.9	0.0
	$D_{1\%}$ [Gy]	42.3 ± 0.3	41.8 ± 0.3	**0.5**
	SD [Gy]	1.1 ± 0.1	1.0 ± 0.1	**0.1**
Body	D_{mean} [Gy]	4.2 ± 1.0	4.0 ± 1.0	**0.2**
	$D_{2\%}$ [Gy]	40.4 ± 0.4	40.2 ± 0.4	**0.2**
Heart	D_{mean} [Gy]	0.7 ± 0.2	0.6 ± 0.1	**0.1**
	$D_{2\%}$ [Gy]	1.8 ± 0.4	1.9 ± 0.6	−0.1
Contralateral	D_{mean} [Gy]	0.3 ± 0.1	0.2 ± 0.1	**0.1**
Lung	$D_{2\%}$ [Gy]	0.9 ± 0.4	0.7 ± 0.3	**0.2**
Contralateral	D_{mean} [Gy]	0.5 ± 0.2	0.4 ± 0.2	**0.1**
Breast	$D_{2\%}$ [Gy]	1.7 ± 0.6	1.9 ± 1.3	−0.2
Ipsilateral	$V_{5\text{Gy}}$ [%]	25.4 ± 4.8	28.0 ± 3.7	**−2.6**
Lung	$V_{20\text{Gy}}$ [%]	14.2 ± 2.7	13.7 ± 2.6	0.5
	D_{mean} [Gy]	6.8 ± 1.1	6.8 ± 1.0	0.0
	$D_{2\%}$ [Gy]	38.0 ± 1.1	37.8 ± 1.1	0.2

TABLE 4.7. Mean values ± standard deviations of dose volume parameters for clinical TF plans and KB-ViTAT (Right-side). Bold font indicates significant ($p < 0.05$) differences.

KB-ViTAT vs clinical TF (Left-side)

Organ	*Parameter*	*TF*	*KB-ViTAT*	ΔP
PTV	$V_{95\%}$ [%]	96.6 ± 1.5	96.3 ± 0.9	0.31
	$D_{1\%}$ [Gy]	41.9 ± 0.3	41.8 ± 0.3	**0.1**
	SD [Gy]	1.0 ± 0.3	1.0 ± 0.1	0.0
Body	D_{mean} [Gy]	3.9 ± 0.9	3.6 ± 0.8	**0.3**
	$D_{2\%}$ [Gy]	40.3 ± 0.3	40.1 ± 0.4	**0.2**
Heart	$V_{3\text{Gy}}$ [%]	12.1 ± 6.1	16.5 ± 6.5	**−4.4**
	$V_{16\text{Gy}}$ [%]	4.1 ± 2.1	3.6 ± 2.1	**0.5**
	D_{mean} [Gy]	2.7 ± 0.9	2.7 ± 0.9	0.0
	$D_{2\%}$ [Gy]	27.4 ± 9.9	23.3 ± 9.0	**4.1**
Contralateral	D_{mean} [Gy]	0.3 ± 0.2	0.2 ± 0.1	**0.1**
Lung	$D_{2\%}$ [Gy]	1.1 ± 0.4	1.0 ± 0.4	0.1
Contralateral	D_{mean} [Gy]	0.6 ± 0.3	0.5 ± 0.2	**0.1**
Breast	$D_{2\%}$ [Gy]	2.1 ± 1.2	2.8 ± 1.2	**−0.7**
Ipsilateral	$V_{5\text{Gy}}$ [%]	19.5 ± 5.9	23.8 ± 6.8	**−4.3**
Lung	$V_{20\text{Gy}}$ [%]	11.9 ± 3.9	10.9 ± 4.5	**1.0**
	D_{mean} [Gy]	5.7 ± 1.6	5.7 ± 1.7	0.0
	$D_{2\%}$ [Gy]	37.6 ± 3.1	35.9 ± 5.1	**1.7**

TABLE 4.8. Mean values ± standard deviations of dose volume parameters for clinical TF plans and KB-ViTAT (Left-side). Bold font indicates significant ($p < 0.05$) differences.

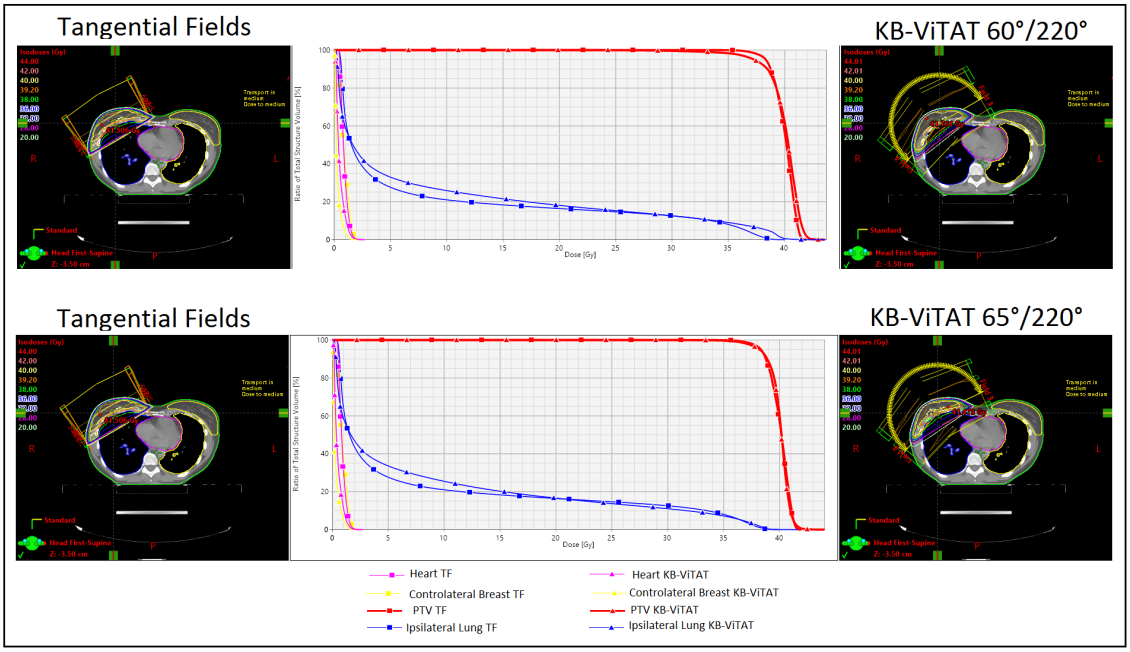

FIGURE 4.8. Right-sided breast treatment example of unacceptable plan using the standard ViTAT configuration. Shifting the medial angle by 5° the plan becomes acceptable in terms of PTV coverage.

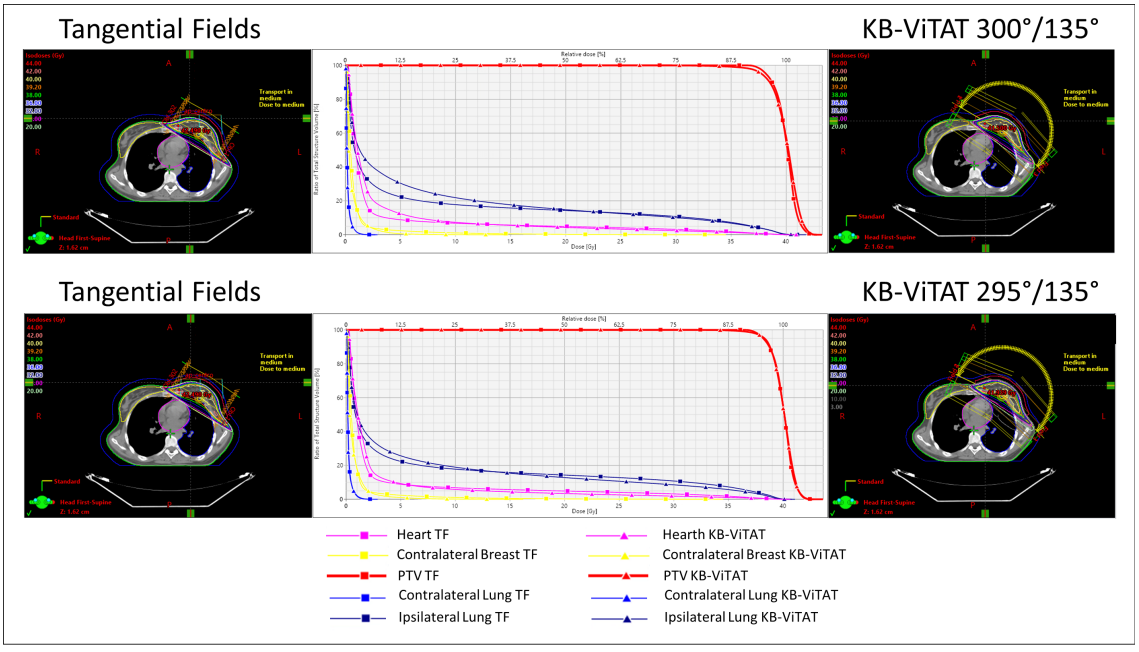

FIGURE 4.9. Left-sided breast treatment example of unacceptable plan using the standard ViTAT configuration. Shifting the medial angle by 5° the plan presents better PTV coverage and better agreement in the ipsilateral lung between KB-ViTAT and TF DVH.

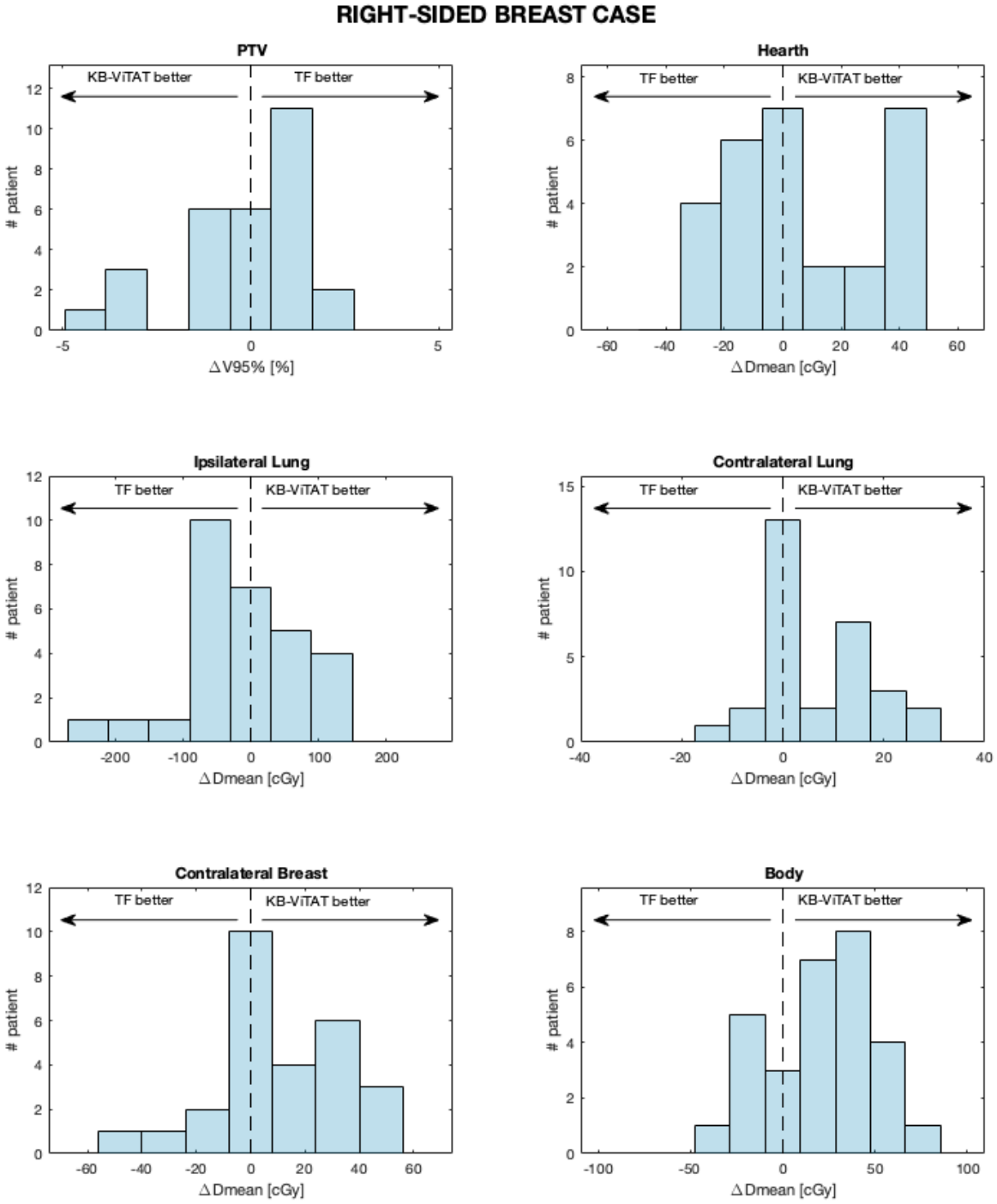

FIGURE 4.10. PTV $V_{95\%}$ and OAR mean doses differences between KB-ViTAT and TF are shown in histograms, highlighting the region where KB or TF plan show better results (Right-sided breast case).

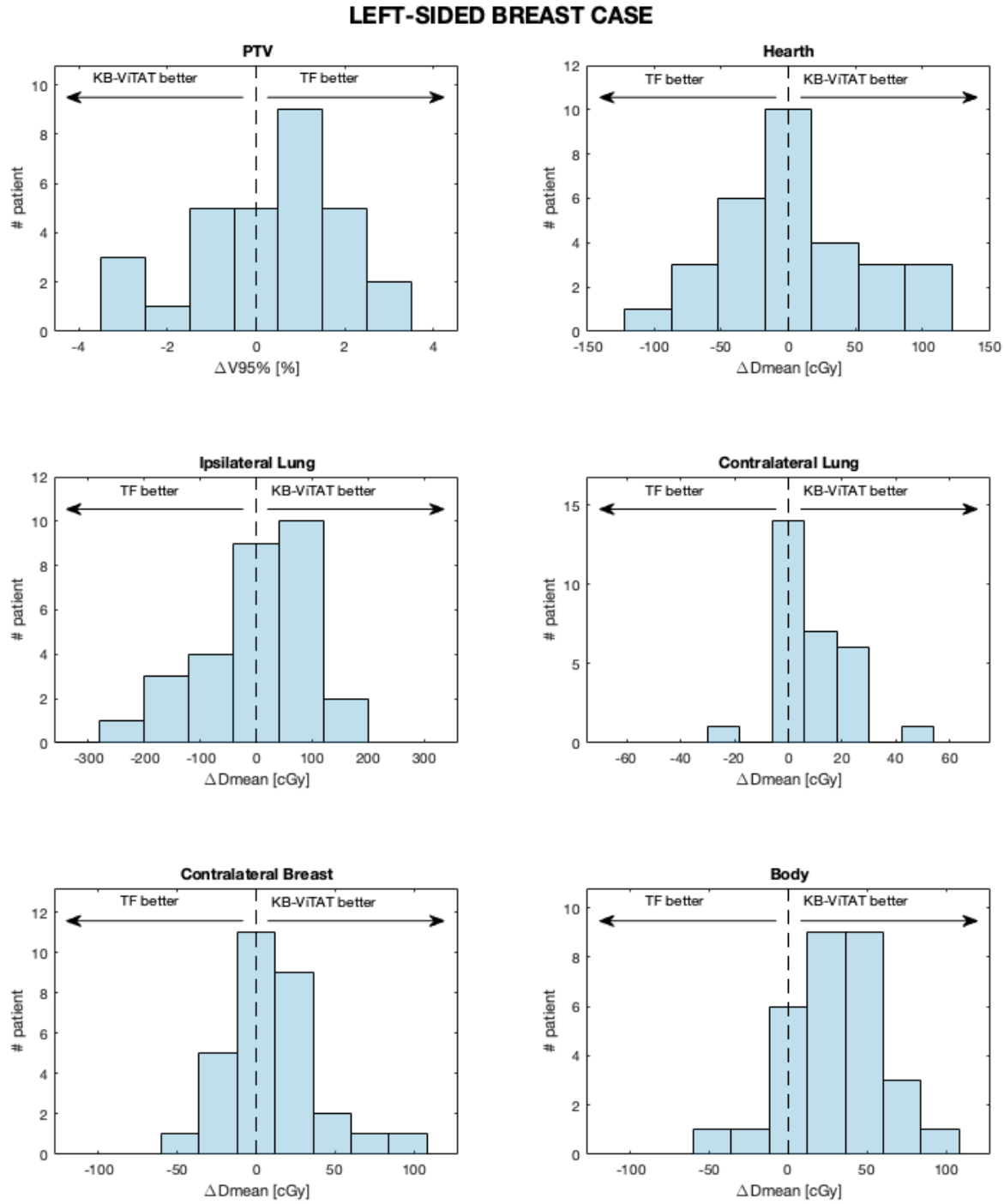

FIGURE 4.11. PTV $V_{95\%}$ and OAR mean doses differences between KB-ViTAT and TF are shown in histograms, highlighting the region where KB or TF plan show better results (Left-sided breast case).

4.3 KB-model in Tomo Direct

4.3.1 ViTAT model in Tomo environment

The KB-ViTAT model performances predicting the outcome DVH are obtained from Figure 4.12 (left) for ipsilateral OARs in terms of point by point differences. The 25% and 75% quantile curves are showing that the KB-ViTAT model is overestimating systematically the predicted DVH. One can be led to a similar conclusion observing Figure 4.12 (right). Here clinical and predicted mean dose for each OAR inside the model were registered and shown. The prediction is obtained considering the mean, the upper and the lower band extracted from the RapidPlan™ tool. Dose volume parameters were extracted from clinical and prediction DVHs, the comparison is reported in Tables 4.9 and 4.10. Significant ($p < 0.05$) differences were found for all OARs: the prediction overestimates ipsilateral lung mean dose up to 1.4 Gy on average, 0.8 Gy for heart (left-case) and up to 0.3 Gy for contralateral breast; ipsilateral lung V_{20Gy} is lower by 4.3% for the right case and 2.8% for the left one; hearth $D_{2\%}$ is overestimated by 7.7 Gy.

4.3.2 Tomo dedicated KB-model generation

The KB model for the TD modality was generated after exclusion of at least one structure for 9 patients, considered to be dosimetric outliers. The obtained R^2 for the contralateral breast is lower than the others because it is not always visible from the BEV of the field, making it difficult for the system to find correlations (see Table 4.11). The regression plots for the ipsilateral OARs are shown in Figure 4.13.

The iterative tests of the five patients allowed to generate the template shown in Table 4.12. The TomoTherapy® template distinguishes between the target structures and OARs. Regarding PTV, the parameters required are the structure importance, the prescription, the minimum dose, the maximum dose and their corresponding structure parameters (priority and importance) and objective penalties distinctively. Other parameters that were tested were the field width, modulation factor and pitch value. The 2.5 cm field was used for the template tests and for internal and external validation, along with a modulation factor of 2.000 and a pitch of 0.251. The number and angle position of beams is equal to the clinical plan, but for new patients it is suggested to use four segments. The optimization calculation grid was set to “fine” to better take into account for hot spots inside and outside the target. The plan was optimized with 350 iterations before blocking the process for final dose calculation. Template translation from Eclipse TPS to Tomo TPS was carried out using the ESAPI code in Figure 4.15.

4.3.3 Model Validation

The validation process was carried out both with patients inside the model (30) and patients outside the model (10). KB-TD plans resulted to be similar or better than what was obtained

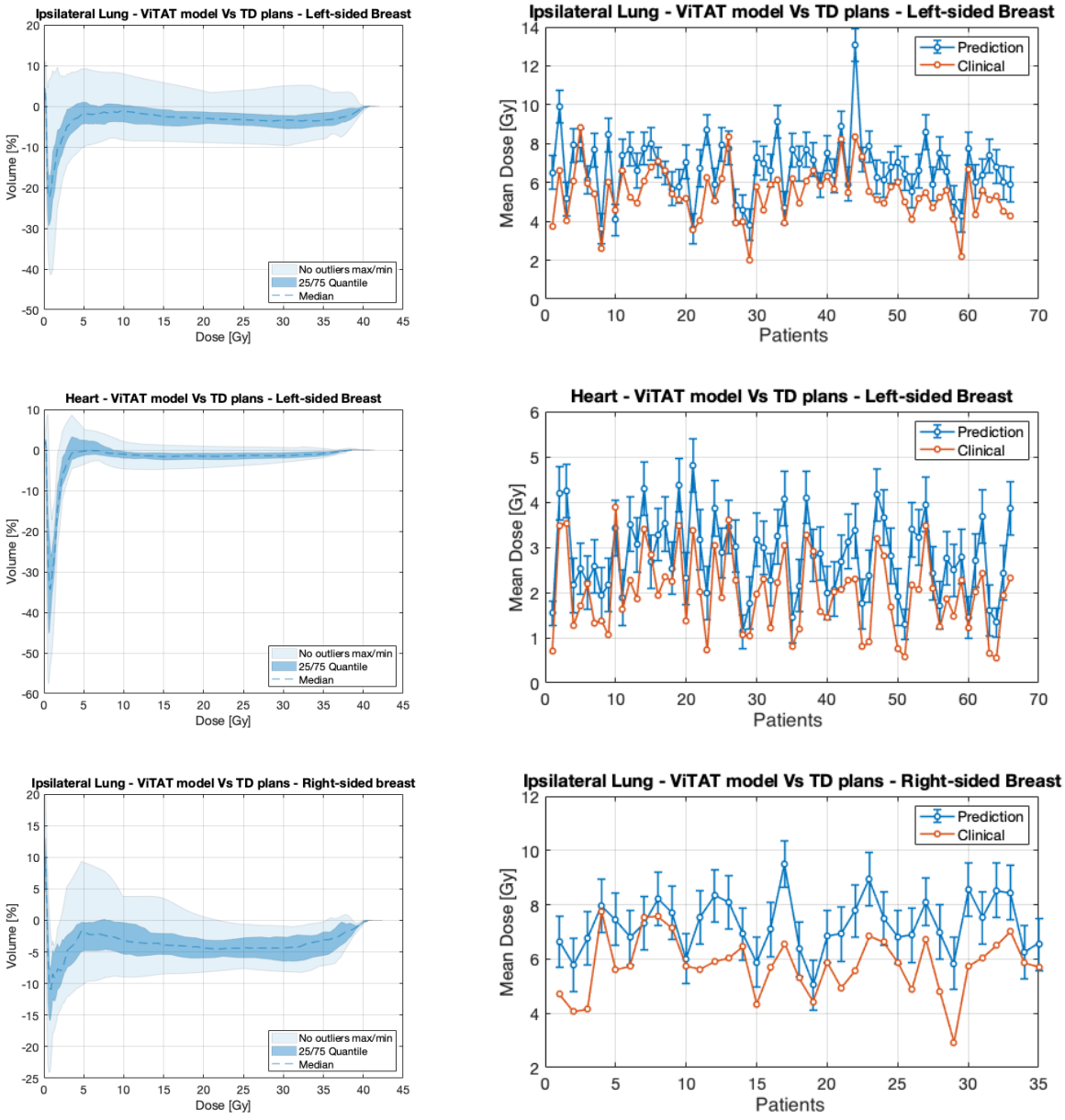

FIGURE 4.12. KB-ViTAT prediction model performances against TD clinical plans for ipsilateral OARs for both Right and Left case. On the left there are the percentage differences calculated point by point over the DVH, shown in terms of quantile 25/75 and maximum and minimum value excluding outliers (using the generalized extreme studentized deviate test). Negative values are associated with a lower value of the clinical plan. On the right: OAR mean doses calculated for the clinical plan (orange points) and for the prediction (blu points). The error bars show the range due to the high and low band prediction of the RapidPlan tool.

ViTAT prediction vs clinical TD - Right-breast Patients				
Organ	*Parameter*	*Clinical*	*Prediction*	ΔP
Ipsilateral	$V_{5\text{Gy}}$ [%]	24.0 ± 5.3	26.2 ± 5.5	**−2.2**
Lung	$V_{20\text{Gy}}$ [%]	11.6 ± 2.6	15.9 ± 2.5	**−4.3**
	D_{mean} [Gy]	5.8 ± 1.1	7.2 ± 1.0	**−1.4**
	$D_{2\%}$ [Gy]	37.0 ± 2.2	38.5 ± 1.0	**−1.5**
Contralateral	D_{mean} [Gy]	0.3 ± 0.2	0.5 ± 0.1	**−0.2**
Breast	$D_{2\%}$ [Gy]	1.4 ± 1.6	2.1 ± 0.4	**−0.7**

TABLE 4.9. Mean values ± standard deviations for Dose volume parameters comparing the ViTAT model prediction against clinical TomoDirect™ plans for Right-breast patients.

ViTAT prediction vs clinical TD - Left-breast Patient				
Organ	*Parameter*	*Clinical*	*Prediction*	ΔP
Ipsilateral	$V_{5\text{Gy}}$ [%]	22.1 ± 5.6	24.1 ± 6.5	**2.0**
Lung	$V_{20\text{Gy}}$ [%]	11.1 ± 3.5	13.9 ± 4.2	**−1.9**
	D_{mean} [Gy]	5.5 ± 1.3	6.8 ± 1.6	**−1.3**
	$D_{2\%}$ [Gy]	36.4± 3.2	37.9 ± 2.6	**−1.5**
Heart	$V_{3\text{Gy}}$ [%]	12.5 ± 10.1	13.3 ± 5.8	**−0.8**
	$V_{16\text{Gy}}$ [%]	2.6 ± 1.9	4.3 ± 2.4	**−1.7**
	D_{mean} [Gy]	2.1± 1.0	2.9 ± 1.0	**−0.8**
	$D_{2\%}$ [Gy]	18.2± 9.5	25.9 ± 11.2	**−7.7**
Contralateral	D_{mean} [Gy]	0.5 ± 0.7	0.8 ± 0.2	**−0.3**
Breast	$D_{2\%}$ [Gy]	2.5 ± 3.3	2.3 ± 0.2	0.2

TABLE 4.10. Mean values ± standard deviations for Dose volume parameters comparing the ViTAT model prediction against clinical TomoDirect™ plans for Left-breast patients.

clinically. Dose-Volume parameters comparison is shown in Tables 4.13 and 4.14 and mean DVHs curves are presented in Figure 4.14.

Internal validation

4 plans out of 30 resulted to be unacceptable in terms of PTV coverage. These plans used only two segments to deliver the dose, while the template and technique was tested using 4 fields. Adding the two missing fields according to the geometry and shifting them by 5° from the previous ones, resulting plans were acceptable and with a better PTV coverage compared to the original clinical plans. The KB approach showed small but significant ($p<0.05$) improvement in the internal validation set: better PTV coverage (1%), improved PTV $D_{1\%}$ (0.4 Gy) and homogeneity (0.09

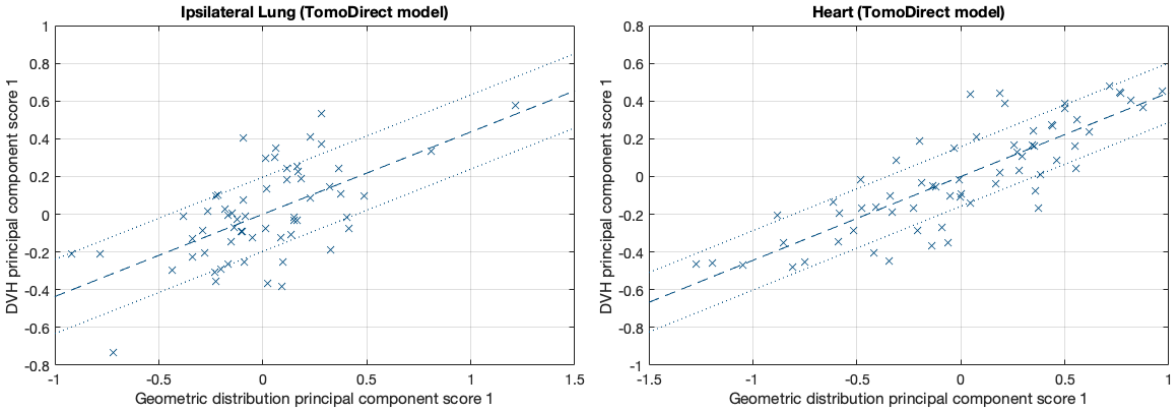

FIGURE 4.13. Regression plots for ipsilateral lung and heart for the TomoDirect™ model for left-sided breast cancer patients.

TomoDirect model - Regression parameters

Structures	χ^2	R^2
Ipsilateral Lung	1.117	0.699
Heart	1.086	0.744
Contralateral Breast	1.047	0.358
Contralateral Lung	1.133	0.842

TABLE 4.11. Regression parameters for the TomoDirect model.

KB-TD Fine -Tuned Optimization Templete

(Priority) Organ	Importance	D_{max} [Gy]	D_{max} penalty	Vol. [%]	Dose [Gy]	Penalty
(T) **PTV**	20	40	55	Median	40	55
(1) **Heart**	4	40	15	Gen.	5	12
				Gen.	16	16
				Gen.	30	15
(2) **Contr. Breast**	3	Gen.	30	Gen.	1	30
(3) **Ipsi. Lung**	4	40	10	Gen.	5	20
				Gen.	20	20
				Gen.	30	12
(4) **Contr. Lung**	2	Gen.	30	Gen.	1	5
(5) **Shell**	5	40	70	7	38	7

TABLE 4.12. Structure priority is in parenthesis next to organ name. PTV is treated as the target (T) structure and prescription is normalized to the median of organ dose. “Gen.” placeholder is automatically replaced with the corresponding value exported from RapidPlan prediction.

TD model - Internal Validation

Organ	*Parameter*	*TD*	*KB-TD*	ΔP
PTV	$V_{95\%}$ [%]	97.1 ± 1.9	98.1 ± 1.3	**−1.0**
	$D_{1\%}$ [Gy]	41.2 ± 0.4	40.8 ± 0.3	**0.4**
	SD [Gy]	0.35 ± 0.13	0.26 ± 0.07	**0.09**
Body	D_{mean} [Gy]	3.6 ± 0.9	3.4 ± 0.8	**0.2**
	$D_{2\%}$ [Gy]	39.8 ± 0.5	39.7 ± 0.4	**0.06**
Heart	V_{3Gy} [%]	9.8 ± 6.0	8.3 ± 4.9	**1.5**
	V_{16Gy} [%]	2.2 ± 1.7	2.1 ± 1.9	0.1
	D_{mean} [Gy]	1.8 ± 0.8	1.7 ± 0.8	**0.1**
	$D_{2\%}$ [Gy]	16.6 ± 9.3	15.2 ± 8.6	1.4
Contralateral	D_{mean} [Gy]	0.21 ± 0.06	0.20 ± 0.05	**0.01**
Lung	$D_{2\%}$ [Gy]	0.62 ± 0.2	0.56 ± 0.15	**0.06**
Contralateral	D_{mean} [Gy]	0.35 ± 0.29	0.26 ± 0.08	**0.09**
Breast	$D_{2\%}$ [Gy]	1.6 ± 2.4	0.8 ± 0.4	**0.8**
Ipsilateral	V_{5Gy} [%]	22.4 ± 4.9	21.0 ± 4.8	**1.4**
Lung	V_{20Gy} [%]	11.2 ± 3.2	10.6 ± 3.5	**0.6**
	D_{mean} [Gy]	5.5 ± 1.2	5.3 ± 1.3	**0.2**
	$D_{2\%}$ [Gy]	36.6 ± 3.3	36.1 ± 3.4	**0.5**

TABLE 4.13. Comparison between clinical TD and KB-TD plans for the internal validation set (30 patients). Bold font is associated with significant differences ($p < 0.05$).

TD model - External Validation

Organ	*Parameter*	*TD*	*KB-TD*	ΔP
PTV	$V_{95\%}$ [%]	96.8 ± 1.0	97.4 ± 1.5	−0.6
	$D_{1\%}$ [Gy]	41.2 ± 0.5	40.9 ± 0.3	**0.3**
	SD [Gy]	0.4 ± 0.1	0.3 ± 0.1	**0.1**
Body	D_{mean} [Gy]	3.7 ± 0.9	3.5 ± 0.9	0.2
	$D_{2\%}$ [Gy]	39.85 ± 0.21	39.82 ± 0.15	0.03
Heart	V_{3Gy} [%]	14.2 ± 9.2	12.2 ± 8.5	2.0
	V_{16Gy} [%]	2.7 ± 1.7	2.9 ± 1.9	−0.2
	D_{mean} [Gy]	2.3 ± 1.0	2.1 ± 0.9	0.2
	$D_{2\%}$ [Gy]	17.3 ± 8.7	18.4 ± 7.9	−1.1
Contralateral	D_{mean} [Gy]	0.21 ± 0.05	0.21 ± 0.04	0.0
Lung	$D_{2\%}$ [Gy]	0.55 ± 0.11	0.54 ± 0.11	0.01
Contralateral	D_{mean} [Gy]	0.31 ± 0.20	0.27 ± 0.13	0.04
Breast	$D_{2\%}$ [Gy]	1.9 ± 2.4	1.1 ± 1.2	**0.8**
Ipsilateral	V_{5Gy} [%]	21.7 ± 2.5	21.3 ± 2.1	0.4
Lung	V_{20Gy} [%]	12.1 ± 1.6	11.2 ± 1.5	**0.9**
	D_{mean} [Gy]	5.7 ± 0.7	5.4 ± 0.6	**0.3**
	$D_{2\%}$ [Gy]	37.8 ± 0.7	37.4 ± 0.9	0.4

TABLE 4.14. Comparison between clinical TD and KB-TD plans for the external validation set (10 patients). Bold font is associated with significant differences ($p < 0.05$).

Gy); Ipsilateral Lung and Heart received a lower mean dose by 0.2 Gy and 0.1 Gy; Contralateral OARs have reduced the mean dose by at least 5% with respect to the clinical TD; integral dose to body was reduced by 0.2 Gy. The delivery time for KB-TD plans averaged over all the 30 patients was 8 ± 1 min that has to be compared with the delivery time of the 5 cm field plans (6 ± 1 min) and the 2.5 cm field plans (8 ± 2 min).

External validation

The lack of availability of more patients treated in TD modality allowed the selection of only 10 other patients for the external validation set. Due to the small number of patients the significance of parameters has been lost with respect to the internal validation case, but it is still possible to see the trend confirming that KB-TD plans quality is equal or slightly better than the TD clinical plans.

KB-TD plans resulted in similar PTV coverage, better PTV $D_{1\%}$ (0.1 Gy, $p < 0.05$) and slightly better PTV homogeneity. There is a reduction of 0.9 Gy and 0.8 Gy to $D_{2\%}$ of ipsilateral lung and contralateral breast, respectively. Since the null hypothesis is not rejected by the analysis, results suggest that the other parameters are not changing significantly in the external validation set between the TD-KB and TD plans populations. The delivery time for KB-TD plans averaged over all the 10 patients population was 8 ± 1 min that has to be compared with the delivery time of the 5 cm field plans (6 ± 1 min) and the 2.5 cm field plans (9 ± 1 min) for the external validation set.

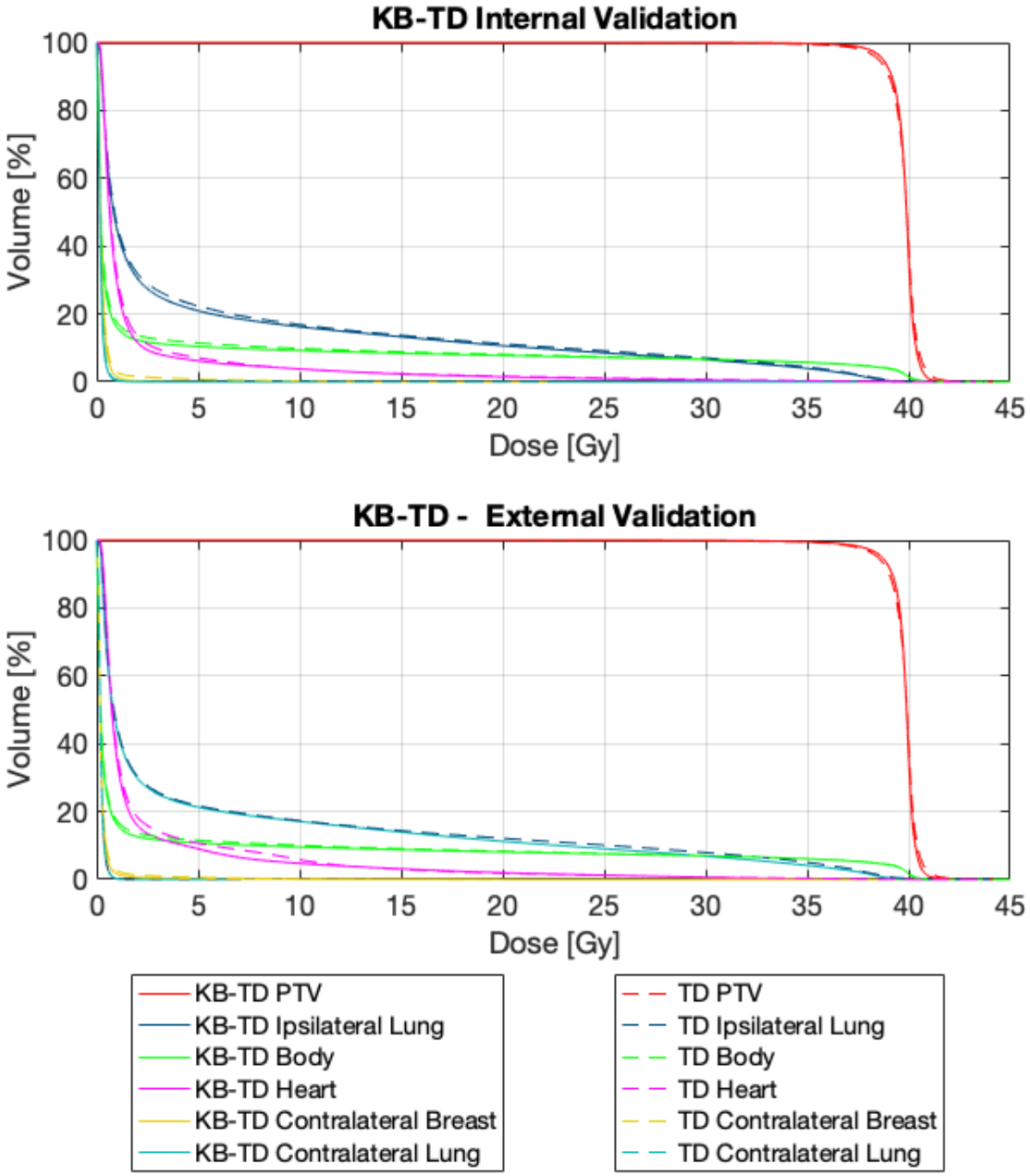

FIGURE 4.14. Mean DVHs for the KB-TD plans (solid lines) and TD ones (dashed lines) for the internal and external validation set.

FIGURE 4.15. Portion of code used to translate the optimization template from Eclipse to Tomotherapy® TPS. This script was embedded in a Microsoft Visual Studio project with a graphic user interface. It generates a readable xml file containing a treating protocol. When a new plan is being created this protocol can be imported and used for plan generation and optimization (Continue in next page).

```
            new string[] {"Volume", "MaxDoseGy","Dose"},  //Mamm Contro
        };

        IEnumerable<OptimizationObjective> objectives = context.PlanSetup.OptimizationSetup.Objectives;

        StringBuilder msg = new StringBuilder();
        int err = 1;
        int structIndex = 0;

        foreach (string id in OARids)
        {
            IEnumerable<OptimizationObjective> templateObjectives = objectives.Where(s => s.StructureId.Equals(id, StringComparison.OrdinalIgnoreCase));
            if (templateObjectives != null && templateObjectives.Any())
            {
                if (structIndex < 2)
                {
                    int parameterIndex = 0;
                    foreach (double parameter in inputParameter[structIndex])
                    {
                        var volumeObj = templateObjectives.First(o => ((OptimizationPointObjective)o).Dose.Dose == parameter);
                        outputParameter[structIndex][parameterIndex] = ((OptimizationPointObjective)volumeObj).Volume;
                        parameterIndex++;
                    }
                }
                else
                {

                    double maxDose = Double.MaxValue;
                    int objectiveIndex = -1;

                    while (true)
                    {
                        try
                        {
                            objectiveIndex++;
                            List<OptimizationObjective> doseObj = templateObjectives.Where(o => ((OptimizationPointObjective)o).Volume == 0).ToList();
                            double tmpObjectiveDose = ((OptimizationPointObjective)doseObj.ElementAt(objectiveIndex)).Dose.Dose;
                            maxDose = tmpObjectiveDose < maxDose ? tmpObjectiveDose : maxDose;
                        }
                        catch
                        {
                            break;
                        }
                    }
                    if (maxDose > 1)
                    {
                        var volumeObj = templateObjectives.First(o => ((OptimizationPointObjective)o).Dose.Dose == inputParameter[structIndex][0]);
                        outputParameter[structIndex][0] = ((OptimizationPointObjective)volumeObj).Volume;
                        outputParameter[structIndex][1] = maxDose;
                    }
                    else
                    {
                        outputParameter[structIndex][0] = 0.01;
                        outputParameter[structIndex][1] = maxDose;
                        outputParameter[structIndex][2] = maxDose-0.01;

                    }

                }
            }
            else
            {

                err = 0;
                msg.AppendLine("struttura '" + id + "' non trovata");

            }

            structIndex++;
        }


        string[][] xmlSructures = prepareXMLstructure(outputParameter, lineXMLPosition, xmlStrings, OARids);
        string[] xmlFileLines = prepareXMLfile(xmlSructures);

        salvaXML(nas_path + Path.DirectorySeparatorChar + "KB_TD_mamm_Sx.xml", xmlFileLines);

        if (err == 1)
        {
            msg.AppendLine("Export del template avvenuto correttamente!");

        }

        MessageBox.Show(msg.ToString());

    }
```

```
1 riferimento | esposito.piergiorgio, 6 giorni fa | 1 autore, 1 modifica
private string[][] prepareXMLstructure(double[][] outputParameters, int[][] whereToModify, string[][] xmlWords, string[] QARids) {
    //"<Volume>##</Volume>"
    //<MaxDoseGy>##</MaxDoseGy>
    string[][] structuresXML = new string[][] {
        //CUORE - 0
        new string[]{
            "<Structure>",
            "<Name>Cuore</Name>",
            "<Type>RAR</Type>",
            "<Display>true</Display>",
            "<Blocked>UNBLOCKED</Blocked>",
            "<Use>true</Use>",
            "<Importance>4</Importance>",
            "<MaxDoseGy>40.0</MaxDoseGy>",
            "<MaxDosePenalty>15</MaxDosePenalty>",
            "<DVH>",
            "<Dose>5.0</Dose>",
            "Vol5",
            "<PointPenalty>12</PointPenalty>",
            "</DVH>",
            "<DVH>",
            "<Dose>16.0</Dose>",
            "Vol16",
            "<PointPenalty>16</PointPenalty>",
            "</DVH>",
            "<DVH>",
            "<Dose>30.0</Dose>",
            "Vol30",
            "<PointPenalty>15</PointPenalty>",
            "</DVH>",
            "<MinDoseGy>0.0</MinDoseGy>",
            "<MinDosePenalty>0</MinDosePenalty>",
            "<OverlapPriority>1</OverlapPriority>",
            "<RGBColor>",
            "<Red>255</Red>",
            "<Green>0</Green>",
            "<Blue>255</Blue>",
            "</RGBColor>",
            "</Structure>"
        },

        //POLMONE SX - 1
        new string[]...,

        //POLMONE DX - 2
        new string[]...,

        //MAMMELLA CONTRO - 3
        new string[]...
    };

    string[][] newStructuresXML = structuresXML;

    for (int structIndex = 0; structIndex < 4; structIndex++)
    {
        int numberOfZeroParameters = 0;
        for(int parameterIndex = whereToModify[structIndex].Length-1; parameterIndex >= 0; parameterIndex--)
        {
            double tmpOutput = outputParameters[structIndex][parameterIndex];
            if (tmpOutput < 0.01)
            {
                numberOfZeroParameters++;
                tmpOutput = numberOfZeroParameters * 0.01;
            }
            newStructuresXML[structIndex][whereToModify[structIndex][parameterIndex]] = "<"+ xmlWords[structIndex][parameterIndex] + ">" + tmpOutput + "</"+ xmlWords[structIndex][
        }
    }

    return newStructuresXML;

}
1 riferimento | esposito.piergiorgio, 6 giorni fa | 1 autore, 1 modifica
private static string[] prepareXMLfile(string[][] structuresXML)
{
    return newStructuresXML;

}
1 riferimento | esposito.piergiorgio, 6 giorni fa | 1 autore, 1 modifica
private static string[] prepareXMLfile(string[][] structuresXML)
{
    string[] xmlFront = new string[] {
        "<?xml version=\"1.0\" encoding=\"UTF-8\"?>",
        "<Protocols>",
        "<Type>Protocol</Type>",
        "<Default>false</Default>",
        "<Protocol>",
        "<Name>KB_TD_mamm_Sx</Name>",
        "<Default>false</Default>"
    };
    string[] xmlBack = new string[]...;

    string[] finalXMLfile = new string[
                                    xmlFront.Length +
                                    structuresXML[0].Length +
                                    structuresXML[1].Length +
                                    structuresXML[2].Length +
                                    structuresXML[3].Length +
                                    xmlBack.Length
                                    ];
    int c = 0;
    xmlFront.CopyTo(finalXMLfile, c);
    structuresXML[0].CopyTo(finalXMLfile, c = xmlFront.Length);
    structuresXML[1].CopyTo(finalXMLfile, c += structuresXML[0].Length);
    structuresXML[2].CopyTo(finalXMLfile, c += structuresXML[1].Length);
    structuresXML[3].CopyTo(finalXMLfile, c += structuresXML[2].Length);
    xmlBack.CopyTo(finalXMLfile, c+= structuresXML[3].Length);

    return finalXMLfile;
}

1 riferimento | esposito.piergiorgio, 6 giorni fa | 1 autore, 1 modifica
private static void salvaXML(string fileFullPath, string[] xmlLines)
{
    using (StreamWriter writer = new StreamWriter(fileFullPath))
    {
        foreach(string line in xmlLines)
            writer.WriteLine(line);
    }
}

}
}
```

CHAPTER 5

DISCUSSION AND CONCLUSION

This thesis was focused on the implementation of KB approaches to automate the plan optimization process for whole breast irradiation. Initially an investigation on inverse-planned VMAT technique development (named VITAT) was carried out. ViTAT was implemented to mimic the performances of the widespread TF, which use manually or inversely optimized segments. [8, 9, 11] The technique was developed with the aim to reduce the intermediate-low dose-spread typical of rotational techniques. [12, 13, 104] Setting properly the geometric parameters, ViTAT generated dose distributions comparable to the TF ones. Results showed some improvement in PTV coverage and homogeneity, better sparing of contralateral OARs and a mild reduction of the integral body dose. On one hand, because of inverse-planning, the ViTAT optimizer algorithm has the intrinsic capability to improve PTV coverage and homogeneity, being the software guided toward this direction. On the other hand, since a consistent amount of plans were realized using physical wedges, ViTAT technique allowed to further reduce the low dose spread for contralateral OARs, due to scattering of photons in wedges, moreover smaller segments were used.

The relationship between the low dose-spread to OARs far from PTV and the increase in risk of secondary radiation-induced malignancies is controversial; for this reason clinicians often prefer to limit or even avoid the use of VMAT techniques in treating whole breast irradiation. [2, 12, 36, 105]

Various authors have proposed a partial VMAT irradiation, blocking the delivery along the arc, trying to compromise between better conformity and OARs sparing for high doses. [33–36] The novelty of this study is the goal of mimicking TF irradiation: in our approach ViTAT uses a smaller portion of the arc of 20°. The chosen delivery methodology depends on the available technology and its implementation could need adaptations to other systems.

A possible alternative consists in dividing the four arcs for each 20° irradiation, generating eight small arcs being delivered in about 5 s instead of 40 s. This solution may be applied in case of breath hold techniques where the time needed to deliver a field is a priority. We preferred our solution to limit the expected stress to the gantry. The total time spared going from the 4-arc solution to the 8 (small)-arc approach would be around or less than 1 min, taking into account both the spared time from the beam-off-rotation and the wasted time due to check and set-up procedure before delivering each arc.

ViTAT still presents some limitations in fully avoiding the low-dose spread in ipsilateral OARs: results showed slight worsening (3-4% volume on average) compared to TF in the range 2-15 Gy. However, these differences were milder with respect to other partial blocked arc approaches and they were likely to be of scarce clinical meaning. Mean dose was in any case unchanged due to an improvement in dose distribution for higher doses.

Once assessed that the ViTAT technique was deliverable and capable of mimicking TF irradiation, we focused on the possibility of using RapidPlan™ tool to handle dose distributions not delivered through an inverse-planning approach. In addition, we explored how to translate the DVH estimation into a functional fine tuned template for fully automatic ViTAT planning. All this resulted in huge improvements in efficiency, reducing inter-planner variability and avoiding suboptimal plans. It is important to notice that about 15% of clinical TF plans were a priori excluded from the training set of the models because they were depicted as suboptimal.

The automatic KB-ViTAT workflow, involving the fixed selection of the start and stop angles, had proven to be an efficient way to mimic TF performances. It failed in about 13% of cases (eight out of sixty plans) resulting in unacceptable PTV coverage and ipsilateral constraints. Seven out of eight plans referred to the left-sided breast case, being more challenging in angle selection due to the presence of the heart. Interestingly, these plans well fitted TF DVHs when manually refining the start and stop angles of the arc by a small amount and relaunching the optimization process. The biggest pro in using an automated technique is the sparing of planning time. With our system and TPS version, a plan is realized in 12 ± 2 minutes including the overall time for automatic plan optimization and dose calculation.

It is worth underlining that the automatic approach proposed here uses a commercially available tool making its potential adoption easy for Varian users, reducing the repetitive manual procedures usually followed during whole breast plan optimization.

The RapidPlan™ tool permits exporting models and sharing them with other institutions, making its application spread potentially easy among other centers. The Multi-Institutional Knowledge-based Approach to Plan Optimization for the Community (MIKAPOCo) project is investigating the differences in DVH prediction between several models generated in various Italian Institutes [75], to assess whether it is feasible to generate a joined prediction “supermodel” to be used as a national reference.

The implementation of the RapidPlan™ tool is not restricted to Varian users. As a matter of

fact it is possible to apply RP models also to other techniques and delivery machines. [32, 67] First, we exploited the possibility to use the KB-ViTAT model prediction on TomoTherapy® patients treated in TomoDirect™ modality, without modifying the training set of patients. Results show that for ipsilateral OARs a systematic error (overestimation of 2-4% on average along the whole DVH) may be present most likely due to intrinsic differences of delivery modalities and dose distribution calculation. Therefore, RP was used to generate a dedicated model for TD patients. Template generation remains a sensitive process, especially in our case where the DVH-prediction had to be translated into a template executable by the TomoTherapy® system. The automatic TD approach generated plans with equivalent or slightly better quality in terms of PTV coverage OAR mean doses and low-dose volume parameters. Moreover, user personalization is limited due to the use of a protocol with fixed field width, pitch and modulation factor. The use of two fields is not always associated with the optimal dose distribution, depending on the geometry of patients' anatomy. Therefore four field segments should always be used to obtain acceptable PTV coverage for all patients. The delivery time of KB-TD plans is 8 ± 1 min due mainly to the chosen field width (2.5 cm). 5 cm field clinical plans (65% of historical patients) are delivered in 6 ± 1 min. Despite that, it was necessary to use the 2.5 cm field width to obtain an optimal plan for the remaining 35% of patients using the smaller field width. A smaller field width is associated with a higher conformity of PTV dose distribution. It is expected that the use of our developed KB approach will reduce the planning time and importantly improve the plan homogeneity between planners, avoiding sub-optimal plans. Of note, the ESAPI script developed for the Eclipse system, is an easy and fast method to translate the DVH-prediction into a template readable by the Tomo system. The automatic optimization process lasts for about 20 minutes, but the planner is free to spend this time in other activities.

As future perspectives, the results reported in this thesis could be improved including the Left Anterior Descending (LAD) artery in all prediction models. Right now, it was excluded because the number of LAD-optimized plans where the LAD is contoured is still too small to allow the generation of a good prediction model. Another critical aspect, that has to be further investigated, is the recognition of the patient-specific optimal beam angles, changing correspondingly the arc or the beam for the ViTAT or TD modality. Furthermore the TD model for the right-sided breast case should be implemented when the number of plans is sufficiently high.

In conclusion, the approaches followed here demonstrated the possibility to completely replace the manual tangential and TomoDirect™ breast planning with a knowledge based automatic planning. This approach is versatile and the use of a commercial system is expected to facilitate large-scale implementation.

PUBLICATIONS

The studies reported in thesis have been published in the following articles:

- P. G. Esposito, R. Castriconi, P. Mangili, A, Fodor, M. Pasetti, N. G. Di Muzio, A. del Vecchio and C. Fiorino. *Virtual Tangential-fields Arc Therapy (ViTAT) for whole breast irradiation: technique optimization and validation*. Physica Medica (2020) 77:160-168 https://doi.org/10.1016/j.ejmp.2020.08.011

- R. Castriconi, P. G. Esposito, A. Tudda, P. Mangili, S. Broggi, A. Fodor, C. L. Deantoni, B. Longobardi, M. Pasetti, L. Perna, A. del Vecchio, N. G. Di Muzio and C. Fiorino. *Replacing Manual Planning of Whole Breast Irradiation With Knowledge-Based Automatic Optimization by Virtual Tangential-Fields Arc Therapy*. Frontiers in Oncology (2021) 11:3274 https://doi.org/10.3389/fonc.2021.712423

The paper for the third part of the thesis is still under preparation:

- P. G. Esposito, et al. *Knowledge-Based automatic plan optimization for left-sided whole breast tomotherapy*. (UNDER PREPARATION)

ACKNOWLEDGEMENTS

First of all I would like to thank my co-supervisors Dr. Claudio Fiorino and Dr. Roberta Castriconi for their patience, the precious advices and help they gave me to realize this thesis.

I am grateful as well to Dr. Lorenzo Placidi and Prof. Stefania Pallotta, suggesting various interesting improvements to this work.

Thanks to the whole personnel of Medical Physics and Radiotherapy departments in San Raffaele Institute, especially to Dr. Antonella del Vecchio and Dr. Paola Mangili, who have tutored me along these years.

I completed my formation in the Medical Physics field with the guidance of Prof. Cristina Lenardi and the SSFM staff, to whom I am thankful.

Lastly special thanks are reserved for my parents and my fiancé for all their support.

The studies in this thesis were supported by an AIRC grant (IG23150).

Acronyms

ABC Acting-Breathing Coordinator
AIRO Associazione Italiana di Radioterapia e Oncologia
API Application Programming Interface

BEV Beams Eye View

CBCT Cone Beam Computed Tomography
CI Confidence Interval
CT Computed Tomography s
CTV Clinical Target Volume

DIBH Deep Inspiration Breath Hold
DRR Digitally Reconstructed Radiography
DVH Dose-Volume Histogram
DVHE Dose-Volume Histogram Estimate

EPID Electronic Portal Imaging Device
ESAPI Eclipse Scripting API

FIF Field-In-Field

GED Geometry-based Expected Dose
GEDVH Geometry-based Expected DVH
gEUD generalized Equivalent Uniform Dose

IGRT Image Guided Radiation Therapy
IMRT Intensity Modulated Radiation Therapy

KB Knowledge-Based
KB-TD KB fully-automatic TD
KB-ViTAT KB fully-automatic ViTAT

MCO Multi-Criteria Optimization
MLC MultiLeaf Collimator
MU Monitor Unit

NAS Network Attached Storage

OAR Organ At Risk
OOF Out-Of-Field

PB-AIO Protocol-based automatic iterative optimization
PCA Principal Component Analysis
PC Principal Component
PTV Planning Target Volume

QA Quality Assurance
QUANTEC Quantitative Analysis of Normal Tissue Effects in the Clinic

RA Rapid Arc
ROI Region Of Interest
RP Rapid Plan
RT Radiation Therapy

SIB Simultaneously Integrated Boost
SD Standard Deviation

TD TomoDirect

TF Tangential Fields

TPS Treatment Planning System

ViTAT Virtual Tangential-fields Arc Therapy

VMAT Volumetric Modulated Arc Therapy

3DCRT 3D Conformal Radiation Therapy

List of Tables

List of Figures

BIBLIOGRAPHY

[1] World Health Organization (2020), *WHO report on cancer: setting priorities, investing wisely and providing care for all. Licence: CC BY-NC-SA 3.0 IGO.*

[2] EBCTCG (2011), Effect of radiotherapy after breast-conserving surgery on 10-year recurrence and 15-year breast cancer death: Meta-analysis of individual patient data for 10 801 women in 17 randomised trials., *Lancet* 378, 1707–1716.
doi:https://doi.org/10.1016/S0140-6736(11)61629-2

[3] Pötter, R., Gnant, M., et al. (2007), Lumpectomy plus tamoxifen or anastrozole with or without whole breast irradiation in women with favorable early breast cancer, *Radiation Oncology Biology Physics* 68, 68.
doi:https://doi.org/10.1016/j.ijrobp.2006.12.045

[4] Livi, L., Meattini, I., et al. (2015), Accelerated partial breast irradiation using intensity-modulated radiotherapy versus whole breast irradiation: 5-year survival analysis of a phase 3 randomised controlled trial, *European Journal of Cancer* 51, 451–463.
doi:https://doi.org/10.1016/j.ejca.2014.12.013

[5] Alford, S. L., Prassas, G. N., et al. (2013), Adjuvant breast radiotherapy using a simultaneous integrated boost: clinical and dosimetric perspectives, *Medical Imaging and Radiation Oncology* 57, 222–229.
doi:https://doi.org/10.1111/j.1754-9485.2012.02473.x

[6] Dellas, K., Vonthein, R., et al. (2014), Hypofractionation with simultaneous integrated boost for early breast cancer: results of the german multicenter phase ii trial (aro-2010-01), *Strahlentherapie Onkologie* 190, 646–653.
doi:https://doi.org/10.1007/s00066-014-0658-5

[7] Whelan, T. J., Olivotto, I. A., et al. (2015), Regional nodal irradiation in early-stage breast cancer, *New England Journal of Medicine* 373, 307–316.
doi:http://dx.doi.org/10.1056/NEJMoa1415340

[8] Chui, C. S., Hong, L., et al. (2002), A simplified intensity modulated radiation therapy technique for the breast., *Medical Physics* 29, 522–529.
doi:https://doi.org/10.1118/1.1460875.

[9] Pignol, J., Olivotto, I., et al. (2008), A multicenter randomized trial of breast intensity-modulated radiation therapy to reduce acute radiation dermatitis., *Journal of Clinical Oncology* 29, 522–529.
doi:https://doi.org/10.1200/JCO.2007.15.2488

[10] Donovan, E., Yarnold, J. R., et al. (2008), An investigation into methods of imrt planning applied to breast radiotherapy, *British Journal of Radiology* 81, 311–322.
doi:https://doi.org/10.1259/bjr/28583675

[11] Smith, W., Menon, G., et al. (2010), Imrt for the breast: A comparison of tangential planning techniques, *Physics in Medicine and Biology* 55, 1231–1241.
doi:https://doi.org/10.1088/0031-9155/55/4/022

[12] Nichols, G. P., Fontenot, J. D., et al. (2014), Evaluation of volumetric modulated arc therapy for postmastectomy treatment., *Radiation Oncology* 9, 66.
doi:https://doi.org/10.1186/1748-717X-9-66

[13] Johansen, S., Cozzi, L., et al. (2009), A planning comparison of dose patterns in organs at risk and predicted risk for radiation induced malignancy in the contralateral breast following radiation therapy of primary breast using conventional, imrt and volumetric modulated arc treatment techniques, *Acta Oncologica* 48, 495–503.
doi:https://doi.org/10.1080/02841860802657227

[14] Darby, S., Ewertz, M., et al. (2013), Risk of ischemic heart disease in women after radiotherapy for breast cancer, *New England Journal of Medicine* 368, 987–998.
doi:https://doi.org/10.1056/nejmoa1209825

[15] Johansen, H., Kaae, S., et al. (2008), Extended radical mastectomy versus simple mastectomy followed by radiotherapy in primary breast cancer. a fifty-year follow-up to the copenhagen breast cancer randomised study., *Acta Oncologica* 47, 633–638.
doi:https://doi.org/10.1080/02841860801989753

[16] Penninkhof, J., Spadola, S., et al. (2017), Individualized selection of beam angles and treatment isocenter in tangential breast intensity modulated radiation therapy, *Radiation Oncology Biology Physics* 98, 447–453.
doi:https://doi.org/10.1016/j.ijrobp.2017.02.008

[17] Jameson, M. G., Holloway, L. C., et al. (2010), A review of methods of analysis in contouring studies for radiation oncology, *Medical Imaging and Radiation Oncology* 54, 401–410.
doi:https://doi.org/10.1111/j.1754-9485.2010.02192.x

[18] Zhu, J., Liu, Y., et al. (2019), Preliminary clinical study of the differences between interobserver evaluation and deep convolutional neural network-based segmentation of multiple organs at risk in ct images of lung cancer, *Frontiers in Oncology* 9, 627.
doi:https://doi.org/10.3389/fonc.2019.00627

[19] Yan, H., Yin, F.-F., et al. (2007), Evaluation of an artificial intelligence guided inverse planning system: Clinical case study, *Radiotherapy and Oncology* 83, 76–85.
doi:https://doi.org/10.1016/j.radonc.2007.02.013

[20] Monz, M., Küfer, K., et al. (2008), Pareto navigation - algorithmic foundation of interactive multi-criteria imrt planning, *Physics in Medicine and Biology* 53, 985–988.
doi:https://doi.org/10.1088/0031-9155/53/4/011

[21] Teichert, K., Süss, P., et al. (2011), Comparative analysis of pareto surfaces in multi-criteria imrt planning., *Physics in Medicine and Biology* 56, 3669–84.
doi:https://doi.org/10.1088/0031-9155/56/12/014

[22] Mitchell, R. A., Wai, P., et al. (2016), Improving the efficiency of breast radiotherapy treatment planning using a semi-automated approach, *Applied Clinical Medical Physics* 18, 18–24.
doi:https://doi.org/10.1002/acm2.12006

[23] Fogliata, A., Nicolini, G., et al. (2015), Performance of a knowledge-based model for optimization of volumetric modulated arc therapy plans for single and bilateral breast irradiation, *PLoS ONE* 10, e0145137.
doi:https://doi.org/10.1371/journal.pone.0145137

[24] Rago, M., Placidi, L., et al. (2021), Evaluation of a generalized knowledge-based planning performance for vmat irradiation of breast and locoregional lymph nodes—internal mammary and/or supraclavicular regions, *PLoS ONE* 16, e0245305.
doi:https://doi.org/10.1371/journal.pone.0245305

[25] Wang, J., Hu, W., et al. (2017), Is it possible for knowledge-based planning to improve intensity modulated radiation therapy plan quality for planners with different planning experiences in left- sided breast cancer patients?, *Radiation Oncology* 12.
doi:https://doi.org/10.1186/s13014-017-0822-z

[26] Purdie, T. G., Dinniwell, R. E., et al. (2014), Automation and intensity modulated radiation therapy for individualized high-quality tangent breast treatment plans, *Radiation Oncology Biology Physics* 90, 688–695.
doi:http://dx.doi.org/10.1016/j.ijrobp.2014.06.056

[27] Marrazzo, L., Meattini, I., et al. (2019), Auto-planning for vmat accelerated partial breast irradiation, *Radiotherapy and Oncology* 132, 85–92.
doi:https://doi.org/10.1016/j.radonc.2018.11.006

[28] Zhao, X., Kong, D., et al. (2012), Automated beam placement for breast radiotherapy using a support vector machine based algorithm., *Medical Physics* 39, 2536–2543.
doi:https://doi.org/10.1118/1.3700736

[29] Wang, W., Purdie, T. G., et al. (2012), Rapid automated treatment planning process to select breast cancer patients for active breathing control to achieve cardiac dose reduction, *Radiation Oncology Biology Physics* 82, 386–393.
doi:https://doi.org/10.1016/j.ijrobp.2010.09.026

[30] Nicolini, G., Clivio, A., et al. (2009), Simultaneous integrated boost radiotherapy for bilateral breast: a treatment planning and dosimetric comparison for volumetric modulated arc and fixed field intensity modulated therapy, *Radiation Oncology* 2, 27.
doi:https://doi.org/10.1186/1748-717X-4-27

[31] Castriconi, R., Fiorino, C., et al. (2020), Knowledge-based automatic optimization of adaptive early-regression-guided vmat for rectal cancer, *Physica Medica* 70, 58–64.
doi:https://doi.org/10.1016/j.ejmp.2020.01.016

[32] Cagni, E., Botti, A., et al. (2017), Knowledge-based treatment planning: An inter-technique and inter-system feasibility study for prostate cancer, *Physica Medica* 36, 38–45.
doi:https://doi.org/10.1016/j.ejmp.2017.03.002

[33] Fogliata, A., Seppälä, J., et al. (2017), Dosimetric trade-offs in breast treatment with vmat technique, *British Journal of Radiology* 90, 20160701.
doi:https://doi.org/10.1259/bjr.20160701

[34] Tsai, P. F., Lin, S. M., et al. (2016), The feasibility study of using multiple partial volumetric-modulated arcs therapy in early stage left-sided breast cancer patients, *Applied Clinical Medical Physics* 13, 3806.
doi:https://doi.org/10.1120/jacmp.v13i5.3806

[35] Yu, A. F. and Jones, L. W. (2016), Breast cancer treatment-associated cardiovascular toxicity and effects of exercise countermeasures, *Cardio-Oncology* 2, 1.
doi:https://doi.org/10.1120/jacmp.v13i5.3806

[36] Virén, T., Heikkilä, J., et al. (2015), Tangential volumetric modulated arc therapy technique for left-sided breast cancer radiotherapy, *Radiation Oncology* 10, 79.
doi:https://doi.org/10.1186/s13014-015-0392-x

[37] Hussein, M., Heijmen, B. J. M., et al. (2018), Automation in intensity modulated radiotherapy treatment planning - a review of recent innovations, *British Journal of Radiology* 91, 20180270.
doi:https://doi.org/10.1259/bjr.20180270

[38] Junga, J. W., Leec, C., et al. (2019), Automatic segmentation of cardiac structures for breast cancer radiotherapy, *Physics and Imaging in Radiation Oncology* 12, 44–48.
doi:https://doi.org/10.1016/j.phro.2019.11.007

[39] Wang, H. and Xing, L. (2016), Application programming in c environment with recorded user software interactions and its application in autopilot of vmat/imrt treatment planning, *Applied Clinical Medical Physics* 17, 189–203.
doi:https://doi.org/10.1120/jacmp.v17i6.6425

[40] Xhaferllari, I., Wong, E., et al. (2013), Automated imrt planning with regional optimization using planning scripts, *Applied Clinical Medical Physics* 14, 176–191.
doi:https://doi.org/10.1120/jacmp.v14i1.4052

[41] Yan, H., F-F Yin, et al. (2003), Fuzzy logic guided inverse treatment planning, *Medical Physics* 30, 2675–2685.
doi:https://doi.org/10.1118/1.1600739

[42] Gintz, D., Latifi, K., et al. (2016), Initial evaluation of automated treatment planning software, *Applied Clinical Medical Physics* 17, 331–346.
doi:https://doi.org/10.1120/jacmp.v17i3.6167

[43] Hansen, C., Bertelsen, A., et al. (2016), Automatic treatment planning improves the clinical quality of head and neck cancer treatment plans, *Clinical and Translational Radiation Oncology* 1, 2–8.
doi:https://doi.org/10.1016/j.ctro.2016.08.001

[44] Hazell, I., Bzdusek, K., et al. (2016), Automatic planning of head and neck treatment plans, *Applied Clinical Medical Physics* 17, 272–282.
doi:https://doi.org/10.1120/jacmp.v17i1.5901

[45] Nawa, K., Haga, A., et al. (2017), Evaluation of a commercial automatic treatment planning system for prostate cancers, *Medical Dosimetry* 42, 203–209.
doi:https://doi.org/10.1016/j.meddos.2017.03.004

[46] Song, Y., Wang, Q., et al. (2016), Fully automatic volumetric modulated arc therapy plan generation for rectal cancer, *Radiotherapy and Oncology* 119, 531–536.
doi:https://doi.org/10.1016/j.radonc.2016.04.010

[47] Hansen, C., Nielsen, M., et al. (2017), Automatic treatment planning facilitates fast generation of high-quality treatment plans for esophageal cancer, *Acta Oncologica* 56, 1495–1500.
doi:https://doi.org/10.1080/0284186X.2017.1349928

[48] Müller, B., Shih, H., et al. (2017), Multicriteria plan optimization in the hands of physicians: a pilot study in prostate cancer and brain tumors, *Radiation Oncology* 12.
doi:https://doi.org/10.1186/s13014-017-0903-z

[49] Kierkels, R., Visser, R., et al. (2015), Multicriteria optimization enables less experienced planners to efficiently produce high quality treatment plans in head and neck cancer radiotherapy, *Radiation Oncology* 10.
doi:https://doi.org/10.1186/s13014-015-0385-9

[50] Wala, J., Craft, D., et al. (2013), Maximizing dosimetric benefits of imrt in the treatment of localized prostate cancer through multicriteria optimization planning, *Medical Dosimetry* 38, 298–303.
doi:https://doi.org/10.1016/j.meddos.2013.02.012

[51] Kamran, S., Mueller, B., et al. (2016), Multi-criteria optimization achieves superior normal tissue sparing in a planning study of intensity-modulated radiation therapy for rtog 1308-eligible non-small cell lung cancer patients., *Radiotherapy and Oncology* 118, 515–520.
doi:https://doi.org/10.1016/j.radonc.2015.12.028

[52] Voet, P., Dirkx, M., et al. (2013), Toward fully automated multicriterial plan generation: A prospective clinical study, *Radiation Oncology Biology Physics* 85, 866–872.
doi:https://doi.org/10.1016/j.ijrobp.2012.04.015

[53] Buschmann, M., Sharfo, A., et al. (2018), Automated volumetric modulated arc therapy planning for whole pelvic prostate radiotherapy, *Strahlentherapie Onkologie* 194, 333–342.
doi:https://doi.org/10.1007/s00066-017-1246-2

[54] Voet, P., Dirkx, M., et al. (2014), Fully automated volumetric modulated arc therapy plan generation for prostate cancer patients, *Radiation Oncology Biology Physics* 88, 1175–1179.
doi:https://doi.org/10.1016/j.ijrobp.2013.12.046

[55] Sharfo, A., Breedveld, S., et al. (2016), Validation of fully automated vmat plan generation for library-based plan-of- the-day cervical cancer radiotherapy., *PLoS ONE* 11.
doi:https://doi.org/10.1371/journal.pone.0169202

[56] G. Della Gala, Dirkx, M., et al. (2017), Fully automated vmat treatment planning for advanced-stage nsclc patients, *Strahlentherapie Onkologie* 193, 402–409.
doi:https://doi.org/10.1007/s00066-017-1121-1

[57] Bijman, R., Sharfo, A., et al. (2021), Pre-clinical validation of a novel system for fully-automated treatment planning, *Radiation Oncology* 158, 253–261.
doi:https://doi.org/10.1016/j.radonc.2021.03.003

[58] Biston, M., Costea, M., et al. (2021), Evaluation of fully automated a priori mco treatment planning in vmat for head-and-neck cancer, *Physica Medica* 87, 31–38.
doi:https://doi.org/10.1016/j.ejmp.2021.05.037

[59] Ge, Y. and Wu, Q. J. (2019), Knowledge-based planning for intensity-modulated radiation therapy: A review of data-driven approaches, *Medical Physics* 46, 2760–2775.
doi:https://doi.org/10.1002/mp.13526

[60] McIntosh, C. and Purdie, T. (2016), Contextual atlas regression forests: Multiple-atlas-based automated dose prediction in radiation therapy, *IEEE Transactions on Medical Imaging* 35, 1000–1012.
doi:https://doi.org/10.1109/TMI.2015.2505188

[61] Sheng, Y., Li, T., et al. (2015), Atlas-guided prostate intensity modulated radiation therapy (imrt) planning, *Physics in Medicine and Biology* 60, 7277–7291.
doi:https://doi.org/10.1088/0031-9155/60/18/7277

[62] McIntosh, C., Welch, M., et al. (2017), Fully automated treatment planning for head and neck radiotherapy using a voxel-based dose prediction and dose mimicking method, *Physics in Medicine and Biology* 62, 5926–5944.
doi:https://doi.org/10.1088/1361-6560/aa71f8

[63] Castriconi, R., Fiorino, C., et al. (2019), Comprehensive intra-institution stepping validation of knowledge-based models for automatic plan optimization, *Physica Medica* 57, 231–237.
doi:https://doi.org/10.1016/j.ejmp.2018.12.002

[64] Delaney, A., Dahele, M., et al. (2017), Knowledge-based planning for stereotactic radiotherapy of peripheral early-stage lung cancer, *Acta Oncologica* 56, 490–495.
doi:https://doi.org/10.1080/0284186X.2016.1273544

[65] Yang, Y., Li, T., et al. (2015), Quantitative comparison of automatic and manual imrt optimization for prostate cancer: the benefits of dvh prediction, *Applied Clinical Medical Physics* 16, 241–250.
doi:https://doi.org/10.1120/jacmp.v16i2.5204

[66] Hussein, M., South, C. P., et al. (2016), Clinical validation and benchmarking of knowledge-based imrt and vmat treatment planning in pelvic anatomy, *Radiotherapy and Oncology* 120, 473–479.
doi:https://doi.org/10.1016/j.radonc.2016.06.022

[67] Castriconi, R., Cattaneo, G. M., et al. (2021), Clinical implementation of knowledge-based (kb) automatic plan optimization for helical tomotherapy, *Practical Radiation Oncology* 11, e236–e244.
doi:https://doi.org/10.1016/j.prro.2020.09.012

[68] Varian medical systems, Inc (2013), *Treatment Planning 13.5 New Features*

[69] Varian medical systems, Inc (2015), *Eclipse Photon and Electron Reference Guide*

[70] Roberta Castriconi, Tesi di Specializzazione, Università degli studi di Milano (a.a. 2017-2018), *Knowledge-based planning optimization strategy for helical-tomotherapy*

[71] Cagni, E., Botti, A., et al. (2018), Pareto-optimal plans as ground truth for validation of a commercial system for knowledge-based dvh-prediction, *Physica Medica* 55, 98–106.
doi:https://doi.org/10.1016/j.ejmp.2018.11.002

[72] Boutilier, J., Craig, T., et al. (2016), Sample size requirements for knowledge-based treatment planning, *Medical Physics* 43, 1212–1221.
doi:https://doi.org/10.1118/1.4941363

[73] Fogliata, A., Wang, P., et al. (2014), Assessment of a model based optimization engine for volumetric modulated arc therapy for patients with advanced hepatocellular cancer, *Radiation Oncology* 9.
doi:https://doi.org/10.1186/s13014-014-0236-0

[74] Fusella, M., Scaggion, A., et al. (2018), Efficiently train and validate a rapidplan model through apqm scoring, *Medical Physics* 45, 2611–2619.
doi:https://doi.org/10.1002/mp.12896

[75] Tudda, A. (2021), Oc-0469 inter-institute variability of kb-models for whole breast irradiation with tangential field, *ESTRO 2021. Proffered papers 28: Automated planning*

[76] Anderson, W. F., Jatoi, I., et al. (2006), Assessing the impact of screening mammography: breast cancer incidence and mortality rates in connecticut (1943–2002), *Breast Cancer Research and Treatment* 99, 333–340. doi:https://doi.org/10.1007/s10549-006-9214-z

[77] GRUPPO DI COORDINAMENTO AIRO MAMMELLA triennio 2017-2019 (2019), *Best Clinical Practice nella Radioterapia dei Tumori della Mammella*

[78] Rancati, T. and Fiorino, C. (2019), Modelling radiotherapy side effects: practical applications for planning optimisation (1st ed.), *CRC Press Taylor and Francis Group* doi:https://doi.org/10.1201/b21956

[79] Bergom, C., Currey, A., et al. (2018), Deep inspiration breath hold: Techniques and advantages for cardiac sparing during breast cancer irradiation, *Frontiers in Oncology* 8. doi:https://doi.org/10.3389/fonc.2018.00087

[80] Hoekstra, N., Habraken, S., et al. (2021), Intrafraction motion during partial breast irradiation depends on treatment time, *Radiotherapy and Oncology* 159, 176–182. doi:https://doi.org/10.1016/j.radonc.2021.03.029

[81] Harris, E. J., Mukesh, M., et al. (2014), A multicentre observational study evaluating image-guided radiotherapy for more accurate partial-breast intensity-modulated radiotherapy: comparison with standard imaging technique, *IMPORT Trials Management Group. National Institute for Health Research. Efficacy and Mechanism Evaluation* 1. doi:https://doi.org/10.3310/eme01030

[82] Michalski, A., Atyeo, J., et al. (2012), Inter- and intra-fraction motion during radiation therapy to the whole breast in the supine position: A systematic review, *Medical Imaging and Radiation Oncology* 56, 499–509. doi:https://doi.org/10.1111/j.1754-9485.2012.02434.x

[83] Goddu, S., Yaddanapudi, S., et al. (2009), Dosimetric consequences of uncorrected setup errors in helical tomotherapy treatments of breast-cancer patients, *Radiotherapy and Oncology* 93, 64–70. doi:https://doi.org/10.1016/j.radonc.2009.07.013

[84] Schubert, L. K., Gondi, V., et al. (2011), Dosimetric comparison of left-sided whole breast irradiation with 3dcrt, forward-planned imrt, inverse-planned imrt, helical tomotherapy, and topotherapy, *Radiotherapy and Oncology* 100, 241–246. doi:https://doi.org/10.1016/j.radonc.2011.01.004

[85] Veronesi, U., Cascinelli, N., et al. (2002), Twenty-year follow-up of a randomized study comparing breast-conserving surgery with radical mastectomy for early breast cancer., *New England Journal of Medicine* 347, 1227–1232. doi:https://doi.org/10.1056/nejmoa020989

[86] Gyenes, G., Rutqvist, L., et al. (1998), Long-term cardiac morbidity and mortality in a randomized trial of pre-and postoperative radiation therapy versus surgery alone in primary breast cancer, *Radiotherapy and Oncology* 48, 185–190. doi:https://doi.org/10.1016/s0167-8140(98)00062-0

[87] Lee, B., Lee, S., et al. (2014), Radiotherapy-induced secondary cancer risk for breast cancer: 3d conformal therapy versus imrt versus vmat, *Journal of Radiological Protection* 34, 325–331.
doi:http://dx.doi.org/10.1088/0952-4746/34/2/325

[88] Mcintosh, A., Read, P. W., et al. (2008), Evaluation of coplanar partial left breast irradiation using tomotherapy-based topotherapy, *Radiation Oncology Biology Physics* 71, 603–610.
doi:https://doi.org/10.1016/j.ijrobp.2008.01.047

[89] Lin, T.-C., Lin, C.-Y., et al. (2020), Automated hypofractionated imrt treatment planning for early-stage breast cancer, *Radiation Oncology* 15.
doi:https://doi.org/10.1186/s13014-020-1468-9

[90] Kim, H., Kwak, J., et al. (2018), Automated field-in-field (fif) plan framework combining scripting application programming interface and user-executed program for breast forward imrt, *Technology in Cancer Research and Treatment* 17, 1–10.
doi:https://doi.org/10.1177%2F1533033818810391

[91] Liu, F.-Y., Dong, Z.-W., et al. (2020), Evaluation of the clinical application of auto-planning module for imrt plans of left breast cancer, *Radiation Physics and Chemistry* 166.
doi:https://doi.org/10.1016/j.radphyschem.2019.108500

[92] Rossi, M., Boman, E., et al. (2018), Dosimetric effects of anatomical deformations and positioning errors in vmat breast radio- therapy, *Applied Clinical Medical Physics* 19, 506–516.
doi:https://doi.org/10.1002/acm2.12409

[93] Lizondo, M., Latorre-Musoll, A., et al. (2019), Pseudo skin flash on vmat in breast radiotherapy: Optimization of virtual bolus thickness and hu values, *Physica Medica* 63, 56–62.
doi:https://doi.org/10.1016/j.ejmp.2019.05.010

[94] Esposito, P. G., Castriconi, R., et al. (2020), Virtual Tangential-fields Arc Therapy (ViTAT) for whole breast irradiation: technique optimization and validation, *Physica Medica* 77, 160–168.
doi:https://doi.org/10.1016/j.ejmp.2020.08.011

[95] Rinaldin, G., Perna, L., et al. (2014), Quality assurance of rapid arc treatments: Performances and pre-clinical verifications of a planar detector (mapcheck2), *Physica Medica* 30, 184–190.
doi:https://doi.org/10.1016/j.ejmp.2013.05.004

[96] Aviles Alpuche, J. E., Codero Marcos, M. I., et al. (2018), Creation of knowledge-based planning models intended for large scale distribution: Minimizing the effect of outlier plans, *Applied Clinical Medical Physics* 19, 215–226.
doi:https://doi.org/10.1002/acm2.12322

[97] Scaggion, A., Fusella, M., et al. (2018), Reducing inter- and intra-planner variability in radiotherapy plan output with a commercial knowledge-based planning solution, *Physica Medica* 53, 86–93.
doi:https://doi.org/10.1016/j.ejmp.2018.08.016

[98] Han, E. Y., Paudel, N., et al. (2016), Estimation of the risk of secondary malignancy arising from whole-breast irradiation: comparison of five radiotherapy modalities, including tomohda, *Oncotarget* 7(16), 22960–22969.
doi:https://doi.org/10.18632/oncotarget.8392

[99] Nagai, A., Shibamoto, Y., et al. (2017), Intensity-modulated radiotherapy using two static ports of tomotherapy for breast cancer after conservative surgery: dosimetric comparison with other treatment methods and 3-year clinical results, *Journal of Radiation Research* 23, 1–8.
doi:https://doi.org/10.1093/jrr/rrw132

[100] Michalski, A., Atyeo, J., et al. (2014), A dosimetric comparison of 3d-crt, imrt, and static tomotherapy with an sib for large and small breast volumes, *Medical Dosimetry* 39, 163–168.
doi:https://doi.org/10.1016/j.meddos.2013.12.003

[101] Varian medical systems, Inc (2015), *Eclipse Scripting API Reference Guide*

[102] Ricotti, R., Ciardo, D., et al. (2017), Intra-fraction respiratory motion and baseline drift during breast helical tomotherapy, *Radiotherapy and Oncology* 122, 79–86.
doi:https://doi.org/10.1016/j.radonc.2016.07.019

[103] Alderliesten, T., Heemsbergen, W., et al. (2018), Breast-shape changes during radiation therapy after breast-conserving surgery, *phiRO* 6, 71–76.
doi:https://doi.org/10.1016/j.phro.2018.05.006

[104] Yin, Y., Chen, J., et al. (2012), Dosimetric research on intensity- modulated arc radiotherapy planning for left breast cancer after breast-preservation surgery, *Medical Dosimetry* 37, 287–292.
doi:https://doi.org/10.1016/j.meddos.2011.11.001

[105] Grantzau, T., Thomsen, M., et al. (2014), Risk of second primary lung cancer in women after radiotherapy for breast cancer, *Radiation Oncology* 111, 366–373.
doi:https://doi.org/10.1016/j.radonc.2014.05.004